REPORT No. 220

COMPARISON OF TESTS ON AIR PROPELLERS IN FLIGHT WITH WIND TUNNEL MODEL TESTS ON SIMILAR FORMS

By W. F. DURAND and E. P. LESLEY
Stanford University

REPORT No. 220

COMPARISON OF TESTS ON AIRPLANE PROPELLERS IN FLIGHT WITH WIND TUNNEL MODEL TESTS ON SIMILAR FORMS

By W. F. Durand and E. P. Lesley

INTRODUCTION

The purpose of the investigation, which is the subject of the present report, was to determine the performance characteristics and coefficients of full-sized air propellers in flight and to compare these results with those derived from wind-tunnel tests on reduced scale models of similar geometrical form.

The full-scale equipment comprised five propellers in combination with a VE–7 airplane and Wright E–4 engine. This part of the work has carried out at the Langley Memorial Aeronautical Laboratory, between May 1 and August 24, 1924, and was under the immediate charge of Mr. Lesley. The model or wind-tunnel part of the investigation was carried out at the aerodynamic laboratory of Stanford University and was under the immediate charge of Mr. Durand.

For the full-scale work power absorbed was determined from calibration curves of the engine, derived both before and after the flight tests were made. Useful work is defined as drag of airplane, without influence of slip stream, times velocity, plus weight times rate of climb; efficiency as useful work divided by power absorbed.

The derived coefficients,

$$C_T=\left(\frac{\text{Thrust}}{\rho\, n^2 D^4}\right),\quad C_P=\left(\frac{\text{Power}}{\rho\, n^3 D^5}\right),\ \text{and}\ \eta\ \text{(efficiency)}$$

are plotted on $\frac{V}{nD}$, and curves are drawn representing the average of plotted spots.

For the model investigation, the corresponding coefficients and elements of the performance were determined by direct measurement of resistance, thrust, torque, air speed, and revolutions, as described in detail in Part II of the report.

A comparison of the curves for full-scale results with those derived from the model tests shows that while the efficiencies realized in flight are close to those derived from model tests both thrust developed and power absorbed in flight are from 6 to 10 per cent greater than would be expected from the results of model tests.

The more detailed description of the equipment employed, the methods of carrying out the observations, and of analyzing and reducing the results will be found in Parts I and II of the report as below.

PART I

FULL-SCALE TESTS

TEST PROPELLERS

The dimensions of the propellers tested are shown in Figures 1 to 5 and Table VIII.

The propellers are of the United States Navy standard plan form. They were made of birch in the usual laminated construction and covered with cotton fabric. The blade angles were measured before tests, and no appreciable difference was found between such measurements and those made by the Navy inspector at the works of the Hartzel Walnut Propeller Co., the angles being found correct within the tolerance allowed by the Navy specifications. At the close of the tests the pitch angles were again measured and the following determined:

Propeller	Mean geometrical pitch
B′	5′−0.4″
D′	6′−2.8″
I	5′−8.5″
K′	5′−8.5″
L′	5′−8.6″

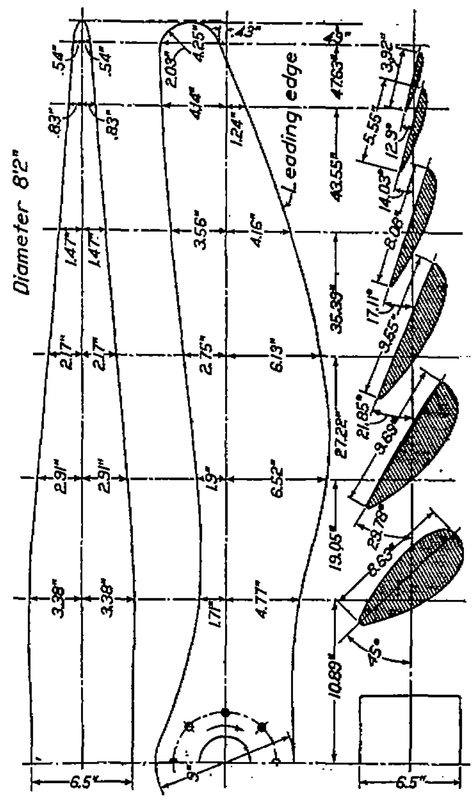

Pitch: 5′ 8.6″. Pitch ratio: 0.7. Aspect ratio: 5. Camber ratio: Minimum + 20 per cent. Rotation: Right hand.

FIG. 1.—Experimental propeller L′ for VE-7 airplane

Propeller B′ is thus seen to have had at the close of the tests appreciably less than the designed pitch of 5′−1.2″. All are believed to have been as nearly geometrically similar to the models, which were made from the same drawings by the application of a linear scale ratio, as is practicable of realization with wood construction.

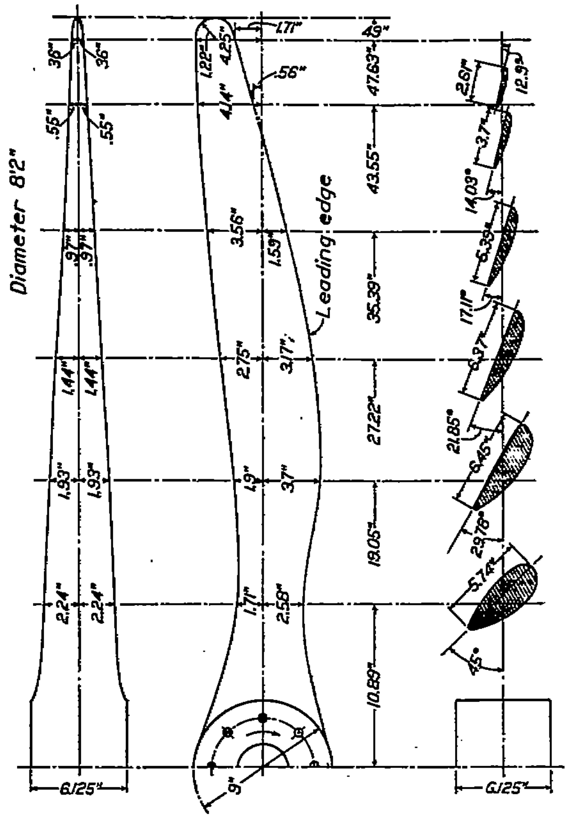

Pitch: 5′ 8.6″. Pitch ratio: 0.7. Aspect ratio: 7.5. Camber ratio: Minimum + 20 per cent. Rotation: Right hand.

FIG. 2.—Experimental propeller K′ for VE-7 airplane

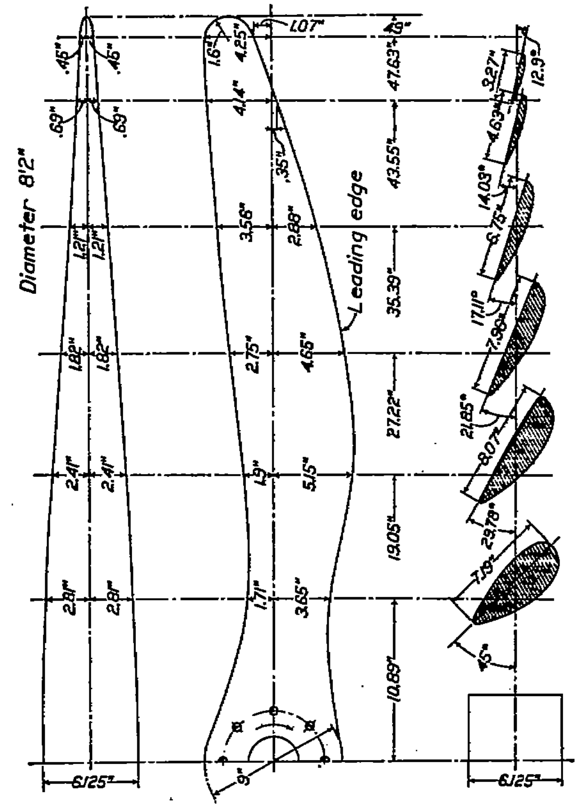

Pitch: 5′ 8.6″. Pitch ratio: 0.7. Aspect ratio: 6. Camber ratio: Minimum + 20 per cent. Rotation: Right hand.

FIG. 3.—Experimental propeller I for VE-7 airplane

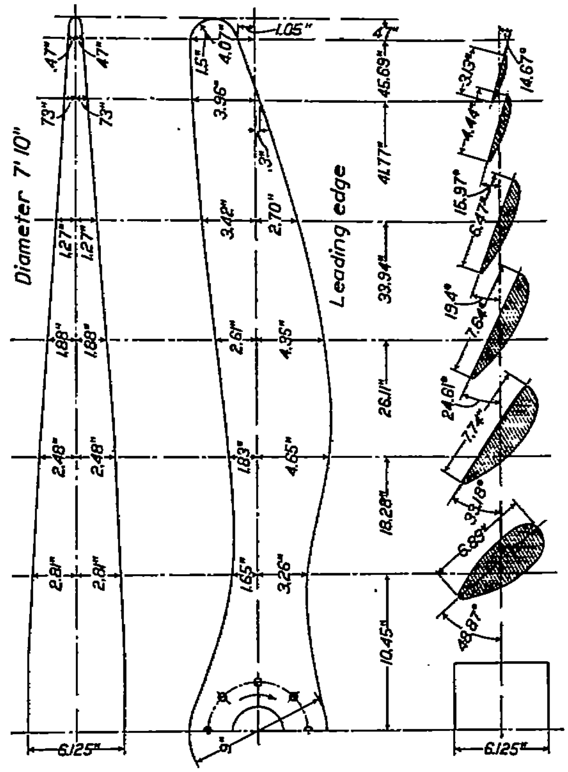

Pitch: 6′ 3.2″. Pitch ratio: 0.8. Aspect ratio: 6. Camber ratio: Minimum + 20 per cent. Rotation: Right hand.

FIG. 4.—Experimental propeller D′ for VE-7 airplane

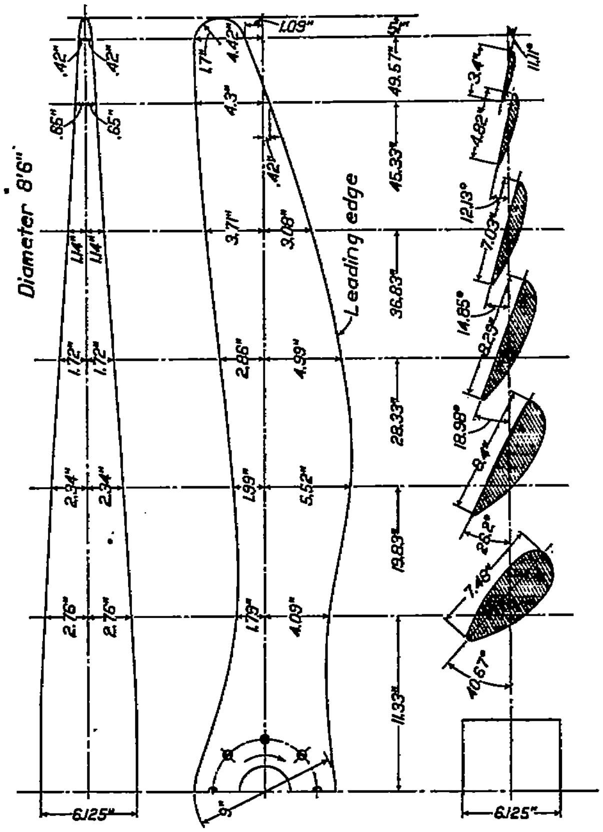

Pitch: 5′ 1.2″. Pitch ratio: 0.6. Aspect ratio: 6. Camber ratio: Minimum + 20 per cent. Rotation: Right hand.

FIG. 5.—Experimental propeller B′ for VE-7 airplane

INSTRUMENTS AND APPARATUS

The instruments and apparatus used in these tests were as follows:

(1) *N. A. C. A. recording altimeter.*

(2) *N. A. C. A. recording pendulum inclinometer and airspeed meter.*—This instrument was fitted with a heavy diaphragm capsule, used for recording the intake manifold depression, in place of the usual airspeed capsule. The pendulum inclinometer, the instrument being rigidly secured to a shelf in the observer's cockpit, gave records of the angle of the wing to the horizontal.

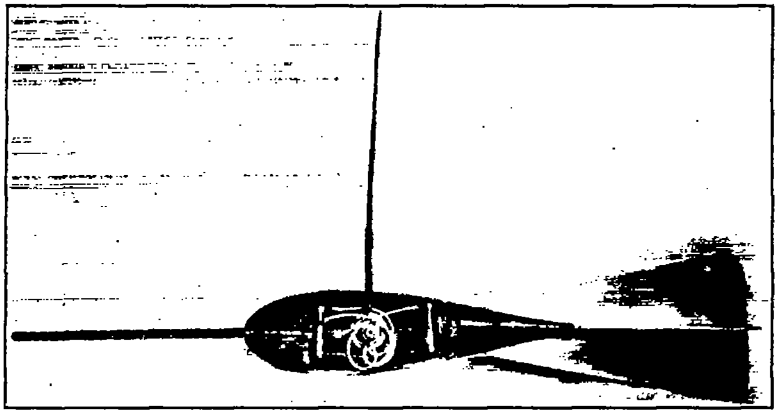

FIG. 6

(3) *A trailing bomb inclinometer and airspeed meter.*—The trailing bomb of this instrument, with cover removed, is shown in Figure 6. It consists essentially of a streamline-form case with stabilizing tail, fitted with a mercury U tube and a Pitot tube. The mercury U tube and Pitot tube are connected, through small rubber tubing and through brass capillary tubing forming the suspending cable, to a pressure diaphragm-type recording instrument placed inside the drum on which the suspending cable is wound. The bomb is suspended from small self-

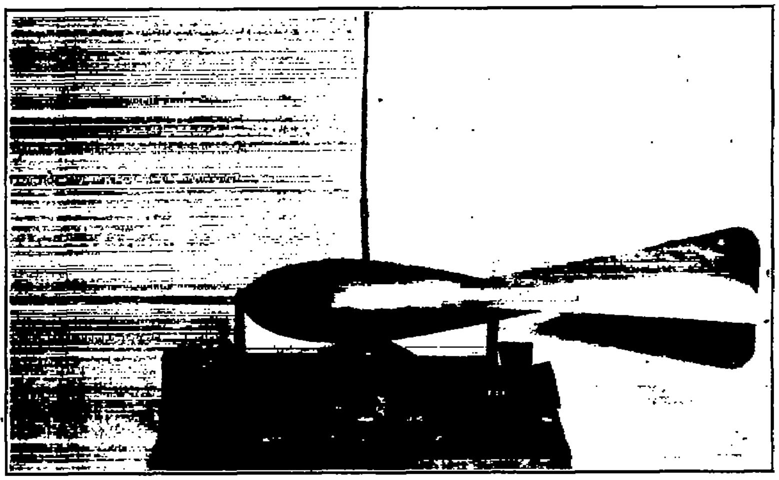

FIG. 7

aligning ball bearings, the bail passing through a longitudinal slot at the top, and is thus free to assume the direction of the air stream flowing by it. Inclination of the bomb from the initial position results in a difference of pressure on the two sides of the diaphragm capsule, to which the mercury U tube is connected, with only a slight displacement of the mercury. The moment of the displacement mercury is balanced by a small righting moment of bomb itself. Thus the bomb remains in any attitude it is placed unless disturbed by some external force. The inclinometer feature is calibrated by placing the bomb in a jig, as shown in Figure 7, tilting to various positions, and making records of the pressures developed at the capsule of the recording manometer.

An equalizing valve is provided in the system, which permits equalizing the pressures on the two vertical legs of the U tube in any desired initial attitude of the bomb. The range of the instrument, with a diaphragm capsule of given sensitivity, is thus doubled. As used in these tests it was provided that a range of 16° could be covered, the instrument being adjusted to record from 0° to 16° of glide, from 0° to 16° of climb, or from 8° climb to 8° glide as desired.

From the record made the angle of flight path is estimated to 0.1°, but the possible error, due to oscillation in flight, inconstancy of recording capsule, and to error in measuring record, appears to be ±0.5°.

A sample record, for gliding flight, is shown in Figure 8. The mean distance of the lighter wavy lines from the base is, from a calibration curve, a measure of the angle of flight path, and the distance of the heavier wavy lines from the same base is a measure of velocity head.

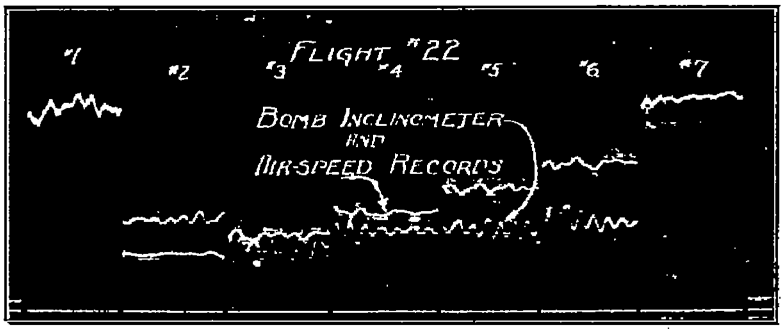

FIG. 8

(4) *Veeder counter.*—This instrument, connected to the engine cam shaft through a simple mechanical clutch, was used to determine engine speed.

(5) *Thermometers.*—Distance-type indicating thermometers were used to determine strut temperature and carbureter intake temperature.

Besides the above, the regular equipment of navigating instruments, such as tachometer, air-speed meter, indicating altimeter, water and oil thermometers, and oil-pressure gage, was installed.

CALIBRATION OF ENGINE

The engine was set up on a Sprague dynamometer test stand for calibration before flight tests, as shown in Figure 9.

During the calibration a 30–70 mixture of benzol and aviation gasoline was used as fuel, the purpose being to avoid danger of incipient detonation at full throttle. In the flight tests, however, it was proposed to use straight gasoline, since this work was to be conducted at such altitudes that the danger of detonation would not exist. This procedure was considered allowable, as it was believed that equal powers would be developed by the mixed and straight fuels under the conditions of flight.

Two carburetor intake temperatures were employed—about 10° and 26° centigrade. On comparison of the brake horsepowers developed in the two cases it was found that, for constant speed and barometric pressure, brake horsepower varied closely as $\frac{1}{\sqrt{T}}$, T being the absolute temperature at the carbureter intake. The mixture control was adjusted, in this calibration, to the full rich position.

Some slight troubles were experienced with one magneto, which finally failed due to breaking of the distributor ring. This magneto, a Splitdorf SS-8, was replaced by a Splitdorf Dixie 800.

After installation in the airplane it was noted that the engine appeared to be rather rough, missing considerably at part throttle, and that, with the airplane on the ground and held stationary, it did not drive the propellers at the speeds expected from model tests, if the power as indicated on the dynamometer were being developed. The fuel used in calibration was substituted for aviation gasoline, but no appreciable improvement in performance could be

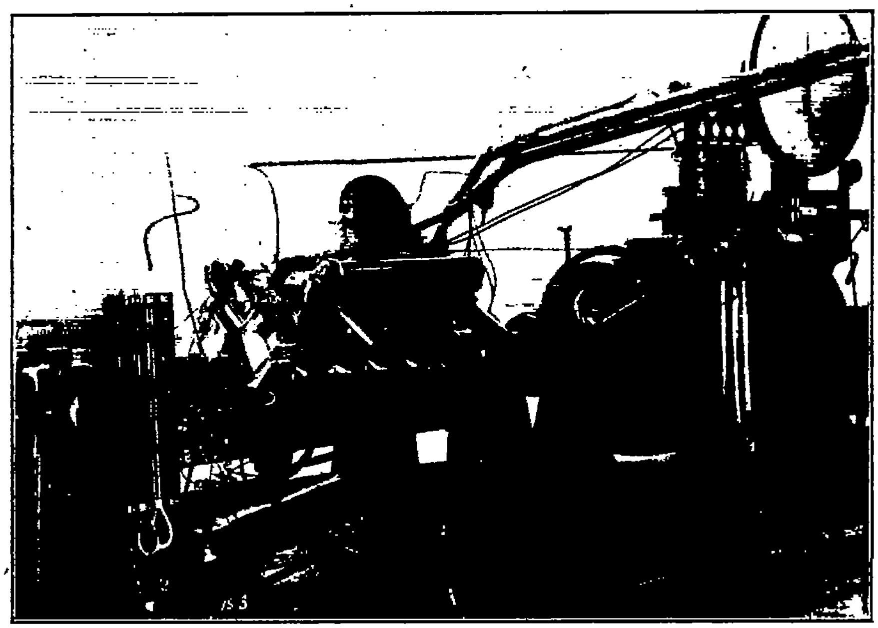

FIG. 9

detected. The installation was therefore checked over, a minor intake manifold leak corrected, the two magnetos used in the calibration replaced by tested accessories (Dixie 800), and the mixture control adjustment wired fast in the full rich position. With these changes the missing was eliminated and the standing R. P. M. at full throttle and with propeller I were observed to be 1,580. The performance with this propeller (standing R. P. M. at full throttle) was thereafter used as an index of engine condition. At no time during the flight tests, which in all occupied about 20 hours running time, was there a change, as shown by the indicating tachometer, of more than 20 R. P. M., the performance being generally consistent.

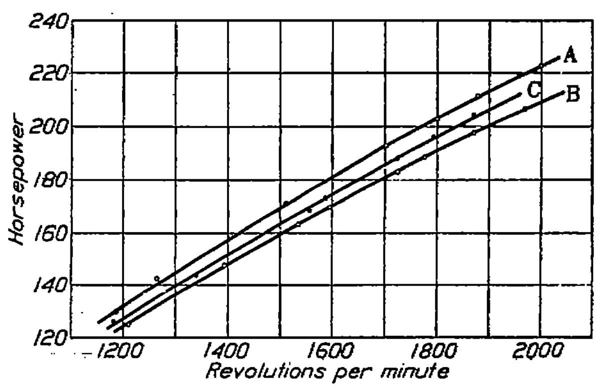

FIG. 10.—Wright E-4 engine calibration reduced to standard air

Curve A—Fuel 30-70 benzol gasoline. Feb. 18, 1924.
Curve B—Fuel gasoline. July 15, 1924.
Curve C—Fuel 30-70 benzol gasoline. July 18, 1924.

At the end of the flight tests the engine was subjected to two further calibrations—first, with aviation gasoline as fuel, and second, with the original 30–70 mixture of benzol and aviation gasoline.

The results of the full-throttle runs of the three calibrations, reduced to the conditions of standard air, are shown in Figure 10. The reduction of the observed data to the conditions of standard air (barometer = 760 mm., temperature = 15.6° centigrade) is accomplished through the assumed relation B.HP. $= C \frac{p}{\sqrt{T}}$, in which p is the barometric pressure, T the absolute temperature at the carbureter intake, and C a constant.

It may be noted that the calibration after flight tests, with aviation gasoline as fuel, shows B.HP. about 6½ per cent less than that before flight tests with the mixed fuel, and that the second calibration with mixed fuel is about 3½ per cent below the first. It appears, then, that between the calibrations, before and after flight tests, the engine deteriorated about 3½ per cent. Since aviation gasoline was used for fuel in the flight tests and many of these were conducted at moderate altitudes (1,500 to 3,000 feet), it also appears that toward the end of the flight tests the power developed by the engine at full throttle may have been little more than that indicated by the lowest calibration curve, while at the start it may have been close to that indicated by the highest curve.

FLIGHT TESTS

The flight tests consisted of, first, a series of glides, with the propeller at approximate R. P. M. for zero thrust, to determine the lift and drag of the airplane at various speeds; and second, power flights with each propeller at speeds covering the practicable range of the airplane, viz, from 50 to 135 miles per hour.

In the glide tests, after climbing to an altitude of about 3,500 feet, the airplane was jockeyed to a condition of steady glide at about 3,000 feet, where the records were started. The range of speed covered was from 50 to 135 miles per hour. The time occupied by each glide, during making of records, was about 40 seconds. In each glide the throttle was closed until the indicating tachometer showed about the R. P. M. for zero thrust at a particular air speed employed, this R. P. M. being determined from a model test of the propeller.

The recording and indicating instruments gave for the gliding flights:

1. True air speed—as determined from the velocity head recorded from the Pitot tube of the trailing bomb and from density of air as derived from altimeter record and strut temperature.
2. Angle of flight path—as recorded by the trailing bomb inclinometer.
3. Angle of wing—as determined from record of pendulum inclinometer.
4. R. P. M.—as determined from Veeder counter attached to engine.

In the glide tests only one propeller (I) was used.

The power flights were made mainly at full throttle and consisted of runs at air speeds from 50 to 135 miles per hour with each propeller; climbing, level flight, or power dives as determined by the speed.

In addition to the full-throttle runs a number of trials at part throttle were made. These were found generally unsatisfactory, however, because of difficulty in maintaining steady conditions, and were discarded. The intake-manifold pressure, from which it was expected to deduce engine power, was found to fluctuate considerably with the slight throttle adjustment necessary to maintain uniform engine speed at a given speed of flight. Then, too, it was found that the range of $\frac{V}{nD}$ that could be covered in level flight was very small, and that at the lower speeds the power required for level flight was so small as to be below the range of the engine calibration.

In the power flights the instruments provided data for:

(*a*) True air speeds—from trailing bomb Pitot and air density as in gliding flight.
(*b*) Angle of flight path.
(*c*) Angle of wing.
(*d*) R. P. M.
(*e*) Intake manifold depression (not used except as indication of throttle opening).
(*f*) Carburetor intake temperature as determined from indicating thermometer.
(*g*) Air density as determined from barometric pressure and strut temperature.

REDUCTION OF DATA

No thrust gliding flights.—The essential observed and computed data for the glide tests are shown in Table I.

The angle of attack is found by subtracting the angle of the flight path from the angle of wing.

The airplane, with fuel, oil, and water and with pilot and observer, was weighed before tests. Allowance is made for fuel, oil, and water consumed in each flight.

Lift is taken as equal to $W \cos \alpha$, α being the angle of the flight path.

The apparent drag is numerically equal but opposite in sign to $W \sin \alpha$.

True drag is apparent drag plus thrust, and thrust is derived from the thrust coefficient of a model propeller for the value of $\frac{V}{nD}$ attained in the glide test, it being rarely possible to realize the exact $\frac{V}{nD}$ for zero thrust (0.972 for propeller I).

$\frac{1}{2}\rho V^2$ is given in the table in pounds per square foot and is derived directly from the record and calibration of the pressure capsule connected to the pitot tube of the trailing bomb.

C_L and C_D are $\frac{\text{Lift}}{\frac{1}{2}\rho V^2 S}$ and $\frac{\text{Drag}}{\frac{1}{2}\rho V^2 S}$ respectively; S being taken as 284.5 square feet.

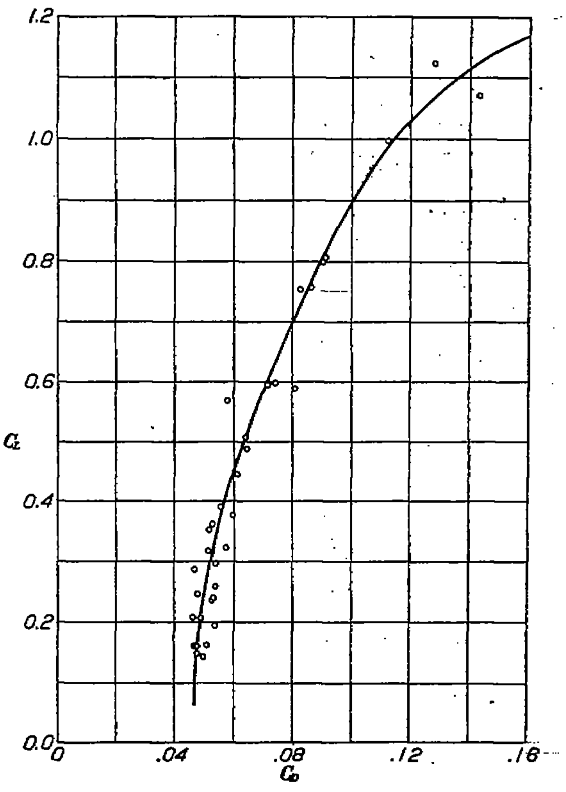

FIG. 11.—Polar diagram of Vought VE-7 airplane

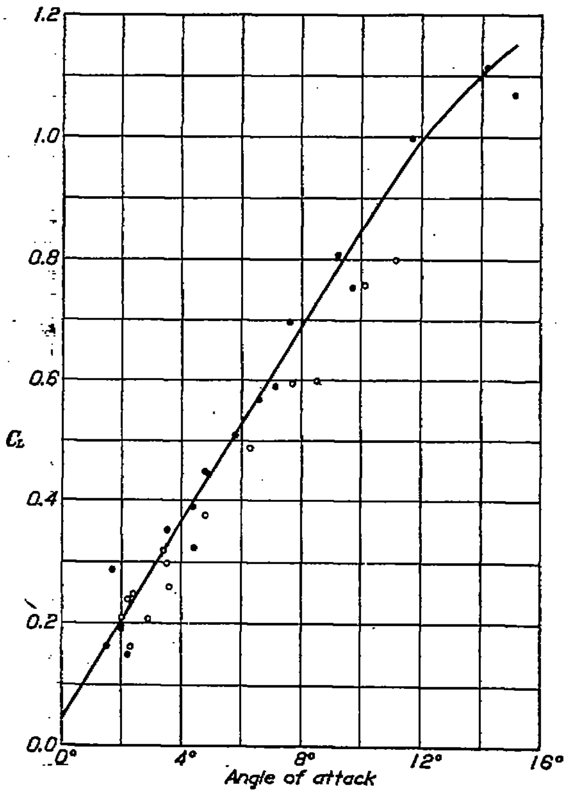

FIG. 12.—Lift characteristic of Vought VE-7 airplane

The final coefficients C_L and C_D, plotted as a polar diagram, are shown in Figure 11, a curve representing a reasonable estimate of the average of points being drawn.

In addition the points for C_L plotted against angle of attack are shown in Figure 12. In drawing a curve for this plot the preference has been given to points determined in the later glides, it being found that in the first flights the pendulum inclinometer was out of adjustment (loose pivots) and the calibration somewhat doubtful.

Power flights.—The essential observed and computed data for the power flights are shown in Table II.

As in the glides, the specific weight of the encountered air is computed from the recorded barometric pressure and the observed strut temperature, the air being regarded as dry. It is realized that the specific weights thus derived are generally somewhat in excess of the correct values, as the air at Langley Field is usually very humid even at an altitude of two or three thousand feet. However, since at ordinary temperatures the difference in weight between dry and saturated air is less than 1 per cent and since the air encountered was obviously intermediate in weight between dry and saturated air, it was felt that regarding the air as dry involved no error of consequence.

Velocity is computed from specific weight and from the velocity head as recorded by the pressure capsule connected to the trailing bomb Pitot.

R. P. M. are found from observations of the Veeder counter.

Angle of flight path is recorded by the trailing bomb inclinometer and angle of wing by the pendulum inclinometer. Angle of attack may be found by taking the difference between the two angles recorded. Because of difficulty in securing consistent records from the pendulum inclinometer, a different method of determining the angle of attack, described later, was used.

Weight is determined as in the no-thrust gliding flights.

Lift, drag, and thrust are determined as follows:

A first approximation or tentative lift L' ($= W\cos\alpha$) is assumed, thus neglecting the lift component of the propeller thrust. From this tentative lift the observed velocity head and the area of the wing surface C'_L (a tentative lift coefficient) is computed. A corresponding C'_D is read from the polar diagram, Figure 11, and a tentative angle of attack from Figure 12. From C'_D a tentative drag is computed. A tentative thrust T', equal to tentative drag plus $W\sin\alpha$, is then deduced. A second approximation of lift is then determined by deducting $T'\sin B$, the lift component of tentative thrust, from the tentative lift. B is the angle of the propeller axis to the flight path and is 2° less than the angle of attack. From this second approximation of lift a new lift coefficient, angle of attack, drag coefficient, and drag are derived.

A second approximation of thrust is determined by adding, as before, $W\sin\alpha$ to the drag.

Trials for a third approximation of drag, deduced in a similar manner, gave values differing from the second approximation by too small an amount to be of practical consequence.

Lift and drag as given in Table II are thus second approximations, and angle of attack is that read from Figure 12 for a lift coefficient derived from the second approximation of lift. Likewise, the thrust of Table II is second approximation of drag + $W\sin\alpha$.

Horsepower is derived from the calibration curves of Figure 10 as follows:

It is first assumed that during the tests the engine changed from the condition as represented by the highest calibration curve to that as represented by the lowest; that such change was gradual and that therefore at any time between the first and last flight the condition would be represented by a calibration curve intermediate between A and B, the space being divided by 32 intermediate lines and these with A and B representing 34 calibrations, each of which would show the condition of the engine for the test flight of the corresponding number. Thus test flight 17 would have a calibration curve halfway between A and B. The early test flights would have calibration curves close to A and the later ones curves close to B. It is found that this method results in less dispersion of points from a smooth power curve than if a single calibration curve is used. In other words, two tests of a given propeller, one conducted at the beginning of the flights and the other at the end, appear more consistent if to the first a calibration curve near to A (fig. 10) is applied and to the second one near to B than they do if a single calibration curve is used for both.

The horsepower for standard air and at the observed R. P. M. is thus determined from the calibration assumed for each flight, and the horsepower for the conditions of flight is derived from this through the assumed relation: $HP. = C\frac{p}{\sqrt{T}}$, p being barometric pressure, T absolute temperature at carbureter intake, and C a constant.

We then have the coefficients as previously defined:

$$C_T=\frac{\text{thrust}}{\rho n^2 D^4}$$

$$C_P=\frac{\text{power}}{\rho n^3 D^5}$$

$$\eta=\text{efficiency}$$

$$=\frac{\text{thrust}\times\text{velocity}}{\text{power}}$$

$$=\frac{C_T}{C_P}\times\frac{V}{nD}$$

Any homogeneous system of units may be employed in deriving the above coefficients.

In Figures 13 to 17 the values of C_T, C_P, and η, derived from the flight tests, are shown as ordinates on abscissas of $\frac{V}{nD}$. Curves are drawn which represent, as nearly as practicable, the average of the experimental spots, while, at the same time, indicating a continuous and consistent relation. Table III shows the values of C_T, C_P, and η, finally chosen as best representing the average of experimental points and through which the curves of Figures 13 to 17 are drawn.

Figures 18 to 22 show the coefficients as derived both from model tests and from full-scale tests, the model tests being those of model propeller in combination with a model plane.

DISCUSSION

At the time these tests were started it was believed that the least reliable data would be those resulting from the estimated performance of an engine under conditions somewhat different from those of calibration. It was thought that thrust, as determined from addition of drag of the airplane and component of weight along the flight path, would be subject to little error. It appears, however, assuming that accurate measurements would result in points falling on smooth curves, as in the case of model tests, that there is little difference in the possible error of the power and thrust determinations, the advantage being somewhat in favor of the former. It is evident from the dispersion of spots that the possible error in a single spot is considerable but it seems likely that the curves drawn in Figures 13 to 17, representing as they do the average of many determinations, should show the performance of the full-scale propellers tested within a very moderate error.

With reference to the apparent greater possible error in thrust, it may be here noted that the thrust as determined is composed of two parts, one due to drag and the other due to component of weight along the flight path. Since the angle of the flight path is uncertain within 0.5 degree, the weight component of thrust may be in error as much as 17 pounds, in some cases amounting to 4 per cent of the total. If to this is added an error in drag, due to initial error in the polar diagram or to observation, the final error in thrust may be considerable.

If the efficiencies given in Table II are plotted, it will be found that the efficiency curves as drawn represent a fair average of the points. The dispersion from a smooth curve is, however, generally greater than for thrust or power. The three curves as drawn are consistent; efficiency being determined by

$$\eta=\frac{C_T}{C_P}\ \frac{V}{nD}$$

Referring to Figures 18 to 22, it may be seen that both thrust and power coefficients as determined from the flight tests are from 6 to 10 per cent more than those derived from model tests, the mean difference being about 8 per cent. The difference appears too consistent and of too great an amount to be chargeable to experimental or accidental error. In the case of

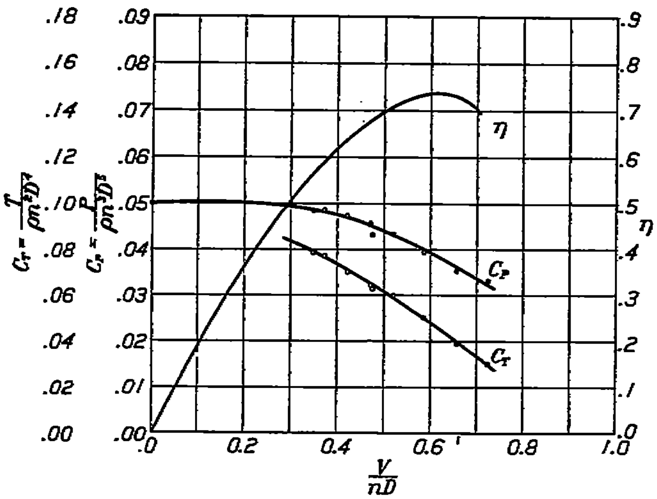

FIG. 13.—Propeller B′ full scale with VE-7 airplane

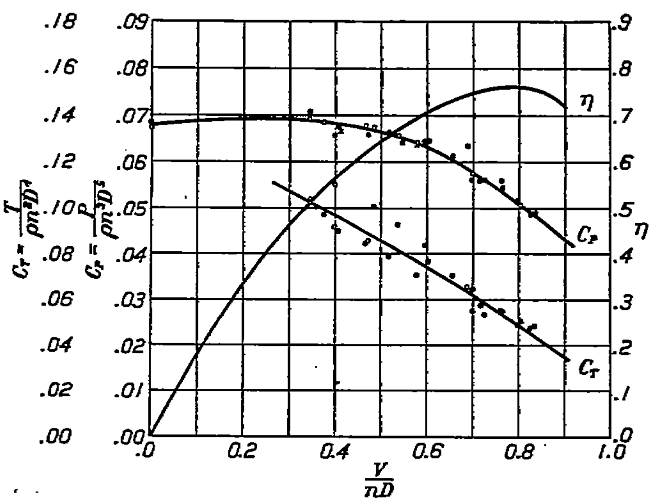

FIG. 14.—Propeller D′ full scale with VE-7 airplane

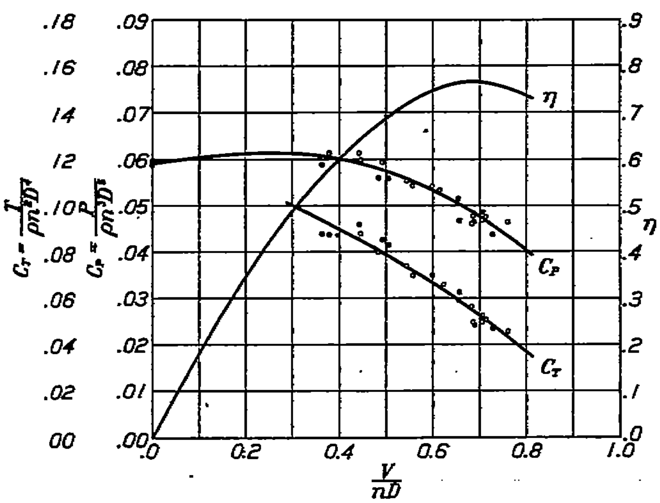

FIG. 15.—Propeller I full scale with VE-7 airplane

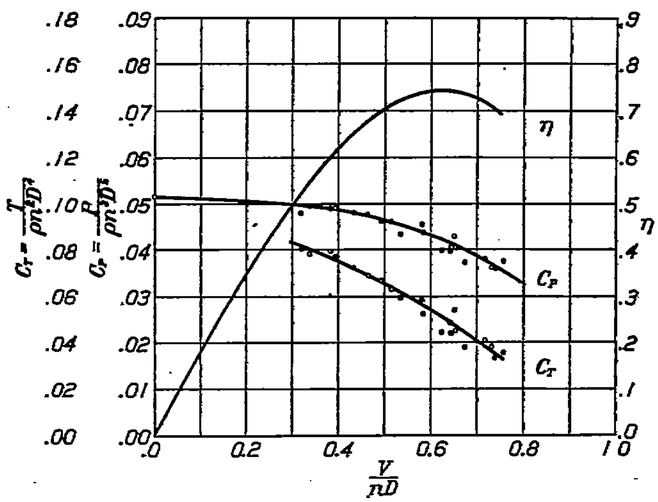

FIG. 16.—Propeller K′ full scale with VE-7 airplane

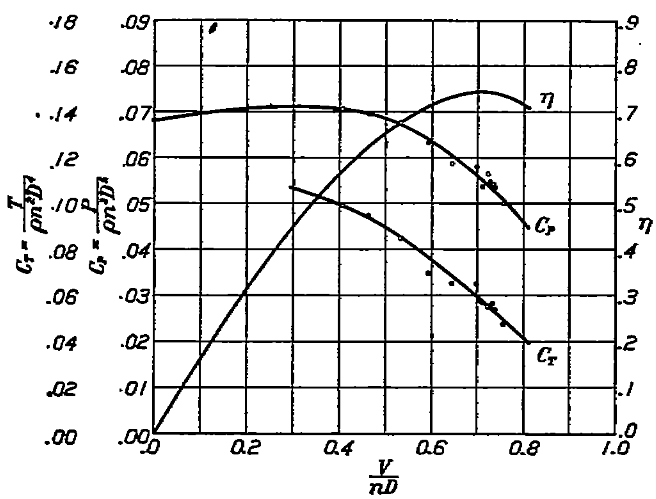

FIG. 17.—Propeller L′ full scale with VE-7 airplane

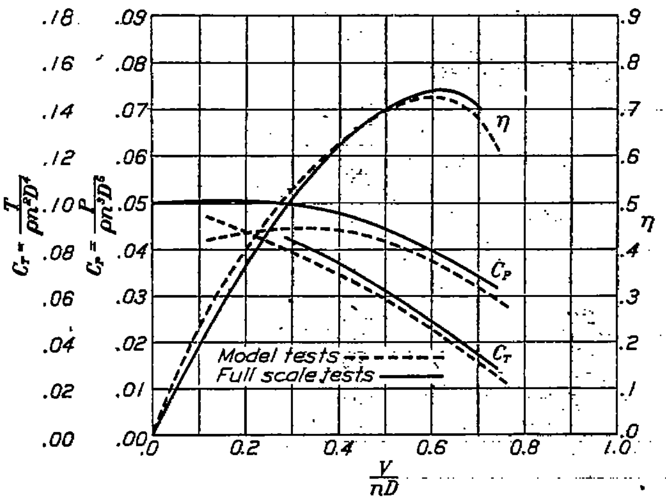

FIG. 18.—Propeller B'

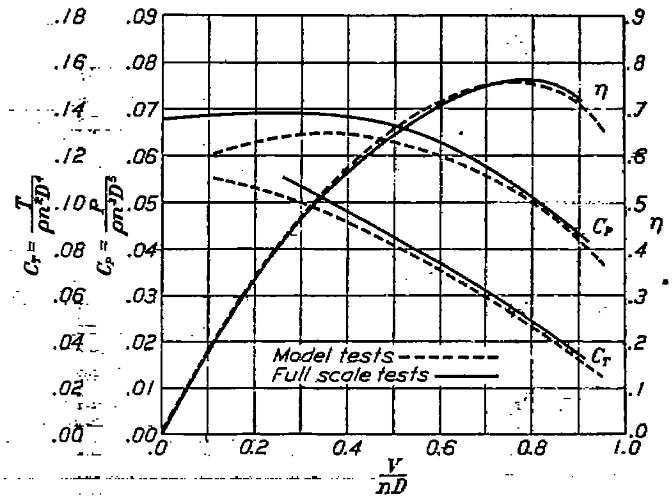

FIG. 19.—Propeller D'

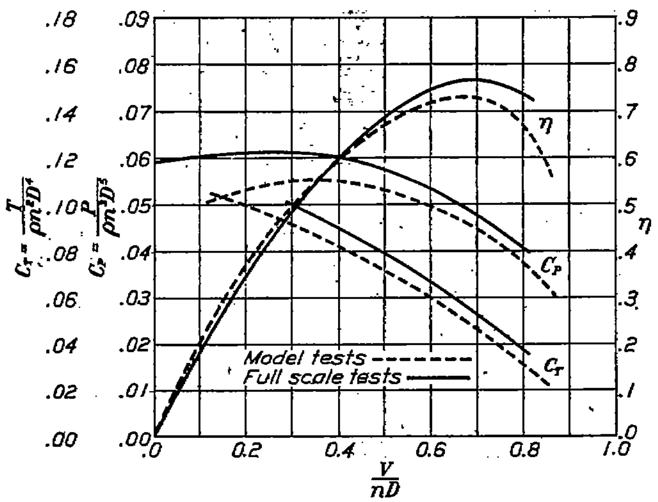

FIG. 20.—Propeller I

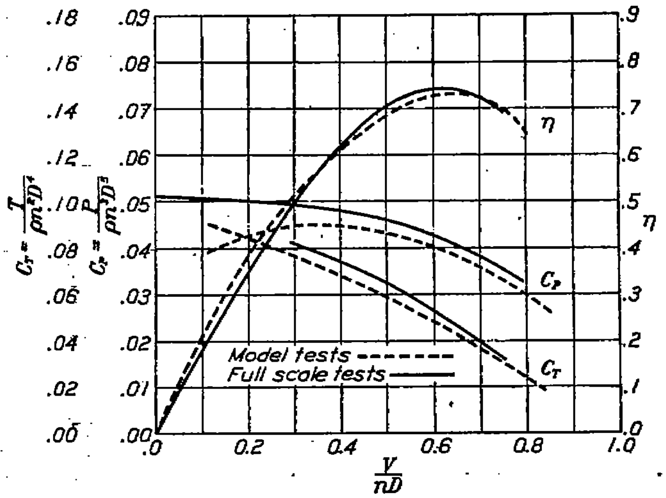

FIG. 21.—Propeller K'

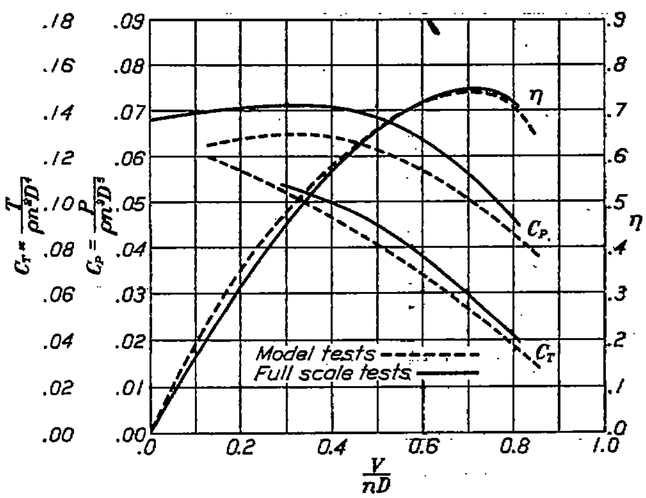

FIG. 22.—Propeller L'

efficiency the difference is considerably less but is also generally consistent. The full-scale propellers show slightly higher peak efficiency than the models and slightly lower efficiency at large slip. The difference is generally less than 3 per cent, in one case only, propeller I, being 4 per cent or more.

There appear to be three possible causes for a somewhat consistent difference between the results of these full-scale and model tests.

1. *Scale effect.*—The linear scale ratio of the full-size propellers and the models is 2.72. The velocity of advance for the flight tests is generally about three times that for the models. The Vl for the sections of the full-size propellers is thus about eight times that for the models, the mean model value being about 50 (ft.-sec. units). If the formula

$$L_{c_2} = L_{c_1} + .057 \log_{10} \frac{v_2 l_2}{v_1 l_1} \text{ (Ref. 1)}$$

is applicable, the increase in lift coefficient for the full-scale propeller sections, due to the higher Vl, would be such as to increase the thrust and power about the 8 per cent experienced.

2. *Difference in the goemetry of the full-scale and model tests.*—In the case of the model propellers the propeller shaft is parallel to the direction of flight. The angle of attack is constant at 2°.

In the flight tests the angle of attack varies between 2° and 12° and the angle of the propeller shaft to the flight path between 0° and 10°. The propeller is thus generally in yaw; only a little at small slip (near peak efficiency) but appreciably at large slip. From such data as are available it appears that the effect of yaw should be to increase both power absorbed and thrust developed. The wider difference between the model and full-scale tests at extreme slip (greater yaw on full-scale) may thus be explained.

3. *Lack of complete similarity of full-scale and model airplanes.*—It will be noted by reference to Figure 24 that in the model airplane the tail surfaces and rear portion of the fuselage are omitted. This was unavoidable with the model propeller dynamometer as constructed. It appears, with respect to power absorbed, that tail surfaces and completed fuselage would have a qualitative effect similar to that of the model as used, but much less in amount. A slight increase in power for small slip and a slight decrease for large slip might thus be expected, as is shown in Part II. However, a considerable body of observation with other models goes to show the very rapid falling off of influence on the propeller with increase of distance between the propeller and the obstructing surface or body, and points definitely to the conclusion that the influence of surfaces giving generally a frictional drag and at distances of one and one-half diameters of the propeller or more would produce an effect on the propeller, presumably within the error of observation.

Likewise it seems unlikely that the slipstream interference offered by the tail surfaces would have any considerable effect upon the shaft thrust as exerted by the model propeller. As is shown in Part II, the thrust credited to the model propeller is equal to the shaft thrust minus the increase or augment of model drag. The shaft thrust might be expected to be larger for the complete model than for the partial model, perhaps by the same order of quantity as with the power. It is not clear what would be the result with regard to the augment of drag, since the slight degree of truncation of the fuselage would tend to offset the influence of the lacking parts of the model, thus perhaps leaving the augment but little changed.

In any case, however, and as noted above, there seems good observational ground for considering the influence of the omitted portions of the model on the propeller performance as presumably within the limit of observational error and in no case apparently sufficient to account for the measurable and consistent difference between model and full-scale results.

Further flight tests and corresponding tests with model propellers and airplanes should be conducted. For the flight tests it is most desirable that simple and reliable thrust and torque meters be developed. The shaft thrust in flight, although not directly applicable to the determination of useful work and consequently of efficiency, would be comparable with a like quantity determined from a model test. The scale effect factor would thus be given a more definite value than if the indirect method of determining thrust, employed in the tests described, is used. The advantage of using a simple and dependable torque meter over relying upon a calibrated engine is obvious.

Indications of somewhat closer agreement between model and full-scale test results are given by model tests conducted at a later date. These tests were too few in number and of insufficient extent to be conclusive and were made too late for inclusion in this report, which was in page proof. They give, however, practically the same power coefficients as previous tests, but thrust coefficients generally somewhat greater, resulting in efficiencies over the working range, from 1 to 3 per cent higher.

It is obvious, in view of the uncertainty in the power developed by the engine, that the power coefficients for the full-scale tests might be made measureably less, and thus the efficiencies for the full-scale propellers also somewhat increased.

The increase in thrust coefficients for the model tests, the decrease in power coefficients for the full-scale tests, and the increase in efficiency for both would tend to bring the full-scale and model results somewhat closer together, and possibly make them as nearly the same as could be expected, considering the experimental errors necessarily involved.

PART II

MODEL TESTS

INTRODUCTION

The model research part of this general investigation was carried on, as noted, at the Aerodynamic Laboratory of Stanford University. There were supplied to the laboratory drawings and specifications for five propellers with dimensions and characteristics as shown in Figures 1 to 5, together with a drawing (fig. 23) showing the central portion of the Vought airplane. The scale ratio between model and full size was 0.3674, thus giving a diameter of close to about 3 feet for the model propellers and of 21 inches for the wing chord of the model plane. The model wings were extended in span on each side approximately 18 inches beyond the blade tips of the propellers, and thus included beyond any question all parts of the model which could in any direct way react with the propeller or be influenced by it. It will also be noted from the scale ratio that this 6 feet of model wing spread represents about 16 feet on the airplane, or some 47 per cent of the total wing spread.

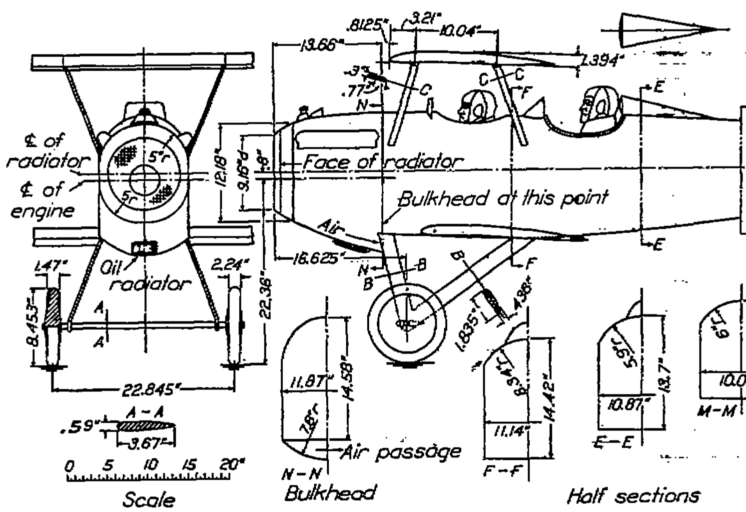

Chord: 20.36". Gap: 20.55". Stagger: 4.13". Angle of wing setting: Upper wing, 1° 45'; lower, 2° 15'.

FIG. 23.—Wing tunnel model of VE-7 airplane

A cut of the model with one of the propellers in position is shown in Figure 24.

Due to the construction of the dynamometer and wind tunnel, the rear extension of the fuselage and tail surfaces were necessarily omitted. The fuselage was faired into the body of the dynamometer with only such clearance as to insure complete freedom under observation.

The fuselage was also hollow, with air entering through the mesh representing the radiator and streaming aft between fuselage and dynamometer body, thus reducing the effect of the truncation at the rear end.

For some comment as to the possible or probable influence of the omitted portions of the model, see Part I, "Discussion."

In an investigation of the character proposed it is clear that the airplane structure, viewed as an obstruction in the wake of the propeller, must also be viewed as a necessary part of the airplane and not as an appendage which might be installed or removed at will.

From this point of view we may develop as follows the form of analysis suited to these conditions.

Assume the model and the propeller in operative relation. The propeller under specified conditions, as determined by a given value of V/nD, develops an actual thrust (pull) T. In so doing, however, it increases the wind reaction of the air on the model by some amount A, which may thus be termed the augment of resistance due to the operation of the propeller. If then from the total thrust T there be subtracted the augment A, there will remain a residual or net thrust $(T-A)$, which alone can be credited to the propeller as a useful final product.

Then if the relative air speed of the airplane is V, the net or useful power will be measured by the product $(T-A)V$. Again, if, in order to realize these conditions, the actual torque and revolutions per second required are Q and n, the input or shaft power will be measured by $2\pi nQ$.

We may then define "propulsive efficiency" as the quotient $(T-A)V \div 2\pi nQ$, and if we denote this efficiency by η we shall have

$$\eta = \frac{(T-A)V}{2\pi nQ}$$

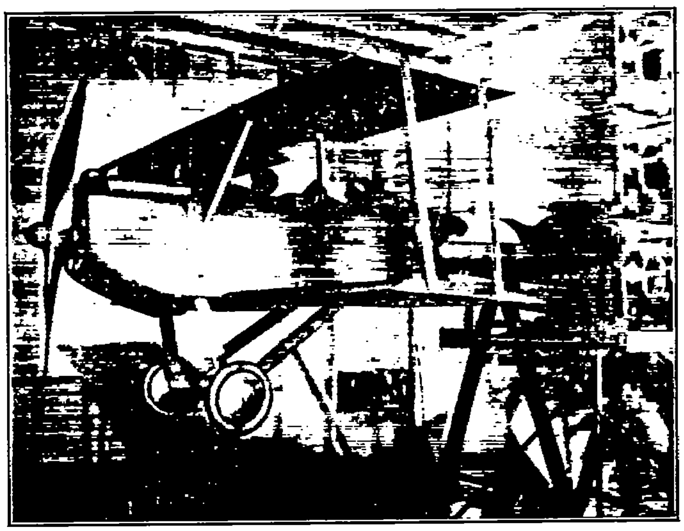

FIG. 24.—Model propeller with model of VE-7 airplane showing method of support

From a slightly different viewpoint we may imagine the propeller at the extremity of a shaft, say 1,000 feet in length, extended out ahead of the airplane. In such case we may assume the interaction between airplane and propeller as nonexistent. Both propeller and airplane will operate as in free air, and the resistance of the latter will be the towed or free-air resistance at the given speed. Likewise the thrust (pull) will equal the resistance, and the propulsive efficiency as defined above (with $A=0$) will be the same as the true propeller efficiency in free air. If then we imagine the shaft to be gradually shortened in, there will begin to develop in due time an interaction between the airplane and the propeller, as a result of which both the thrust (pull) developed and the resistance to be overcome will increase. Finally, with the propeller and airplane in their normal operative relation, we shall find a notable increase in both, and if the engine is driven at such speed as will serve to give the same air speed of the airplane as before, then we may consider that the same net result is accomplished. This useful power will evidently be $(T-A)V$ and the input power to accomplish this will be $2\pi nQ$, the power resulting from the actual n and the actual Q. The ratio between the two will then give the propulsive efficiency under the given conditions of operation as defined by the actual value of V/nD. It should be noted that the value of n and hence of V/nD for a given air speed with the propeller and airplane interacting will not, in general, be the same as that for the ideal case without interaction. The attempt to compare the propulsive efficiency at the value of V/nD in the actual case with interaction with the propeller efficiency at different value of V/nD without interaction greatly complicates the problem, however, and it is believed that for present purposes the comparison of the curve of propulsive efficiency on an axis of V/nD with the corresponding curve of propeller efficiency (free) on its axis of V/nD will show sufficiently well the character and extent of the interaction between the airplane and the propeller in its effect on the efficiency of operation.

In order to realize the condition outlined in the preceding analysis, the program of measurements to be made on the model airplane and propeller must comprise the following:

(1) Wind resistance tests of the model airplane alone.

(2) The usual tests of the propeller alone, giving for a series of values of V/nD values of thrust, torque, and efficiency.

(3) Tests of the combination, including resistance measurements on the model and the usual measurements for the propeller. In the set-up for the test in combination the propeller and model are maintained in their proper geometrical relation but with complete independence of suspension and control, so that all measurements may be made independently and thus give values for the propeller as influenced by the model and for the model as influenced by the propeller.

SET-UP OF APPARATUS AND MODEL

In order to realize this program of measurements, the general character of the apparatus employed with the set-up of the model may be briefly indicated as follows:

It will be recalled that the wind tunnel at Stanford University is of the Eiffel type, with a throat diameter of 7.5 feet and an experiment chamber with a length of 12 feet.

The dynamometer as indicated in the cut of Figure 24 consists essentially of a slender tapering barrel some 9 feet long mounted on knife-edges as a cradle dynamometer and with the model propeller motor located in the larger, down-wind end of the barrel, faired in as a part of the barrel form. The motor is connected to the propeller through a special form of drive which transmits torque with longitudinal freedom. This general arrangement provides for the direct measurement of thrust and torque which are weighed on beam scales graduated, respectively, in hundredths of kilograms and in thousandths of kilogram-meters.

In order to provide for the independent measure of forces on the propeller model and on the airplane model, the latter was suspended by piano wires from the ceiling of the experiment chamber, the length of suspension being about 7 feet. This arrangement is shown in the cut of Figure 24.

For the direct measurement of air forces on the model, a piano-wire bridle was attached to the two sides of the model at shaft level and thus accommodating the propeller between the two sides of the bridle leads. From the apex of the triangle thus formed a single piano wire was led forward (up wind) through the honeycomb baffle, through and beyond the tunnel inlet to the end wall of the building, and over a carefully fitted-up pulley down to a gross weight on the plate of a beam scale weighing to hundredths of a pound. Thus by subtraction the pull on the model due to air flow may be directly weighed on the scale.

In order, however, that the reading of the scale may be made to indicate air forces and nothing else, it is necessary that the model, when in the observing condition, should hang in the free gravity position; otherwise there will be a gravity component, plus or minus, included in the scale reading. In order to eliminate any such component, the following operative routine was followed.

The model, without wind and disconnected from the piano wire leading to the scale, was allowed to hang freely under gravity, and while so hanging a transit instrument, set up abreast of the model and at the side of the experiment chamber entirely out of the wind stream, was adjusted with vertical cross hair on a reference mark on a paper scale attached to the model. Then, during the observations, the model was brought, by suitable fine-motion adjustments, exactly to this initial or zero position, with the mark on the vertical cross hair. Under these conditions the scale readings may be properly interpreted as giving (by subtraction from the gross) the actual wind forces on the model.

It is obvious, furthermore, that this arrangement may be used either with or without the propeller, and thus provide for a measurement of air forces on the model, either in a homogeneous air stream or as influenced by the operation of the propeller placed with any desired clearance between itself and the forward edge or plane of the model.

OBSERVATIONS

In accordance with the general methods indicated in the preceding section, observations were made covering the various elements of the problem. These observations, with the resulting values of the various coefficients, are given in Tables IV and V.

In the reduction of these observations, the following coefficients have been employed:

C_T = thrust coefficient (propeller alone) $= \frac{T}{\rho n^2 D^4}$

C_T = thrust coefficient (propeller with plane) $= \frac{T-A}{\rho n^2 D^4}$

C_P = power coefficient $= \frac{P}{\rho n^3 D^5}$

η = efficiency (propeller alone) or propulsive efficiency (propeller with plane) $= \frac{C_T}{C_P} \frac{V}{nD}$

Graphical representations of these results are shown in the diagram of Figures 25 to 29.

In these diagrams the individual values of the various coefficients are represented by the plotted points. A smooth curve as best indicating a continuous and consistent law is then drawn through and among these spots, and such curve is accepted as the best indication of the law relating the values of the coefficient to varying V/nD. The values of the efficiency η are then derived from the smooth curves of these coefficients and are plotted as shown in the various diagrams. Tables VI and VII give, for various values of V/nD, the values of the coefficients and resulting efficiencies finally chosen as best representing the continuous and consistent law above referred to.

DISCUSSION

(1) It will be noted in all cases that the presence of the obstruction behind the propeller has the effect of moving to the right on the axis of V/nD the point for zero thrust. This condition is readily seen to follow as a result of the slowing down of the column of air actually operative on the propeller as compared with the air passing freely at the side of the obstruction. For any given value of wind velocity as based on the latter the air column acting on the propeller will be slowed down, the value of n for zero thrust will be decreased, and the value of V/nD correspondingly increased.

As will be noted from the diagram, the amount of this shift on the V/nD scale is 0.05 or less for the various propellers employed and for the amount of obstruction represented by the VE–7 model.

(2) From this shift of the point for zero thrust it naturally results that the curve for thrust or thrust coefficient for the combined case as compared with the propeller alone starts farther to the right and near the start lies above that for the propeller alone.

This means that for large values of V/nD the curves for propeller with model will be above that for propeller alone, as noted in the various diagrams. (Figs. 25 to 29.)

As the slip becomes greater, however, and the values of V/nD become less, this excess decreases, and the two curves ultimately meet and cross. For the conditions represented by the present research this point of crossing is seen to be not far from the value of V/nD for best efficiency.

Beyond this point the curve for thrust coefficient lies below that for the propeller alone, thus showing, for this part of the range, a definite loss in value for the propeller in operative position forward of the model.

(3) It thus appears that for large values of V/nD the presence of the model results in a definite increase in the net propulsive effort derived from the propeller, while for moderate and small values the reverse is the case, and, furthermore, that in general the latter condition (loss of net propulsive effort) obtains over that part of the range which must be employed in practical cases.

(4) Similarly, as for the thrust coefficient, the torque, and hence the shaft power coefficient for the propeller with model, is increased for large values of V/nD and decreased for small values, with a crossing point usually at a smaller value of V/nD than for the thrust coefficient. These conditions are plainly seen in the diagrams of Figures 25 to 29.

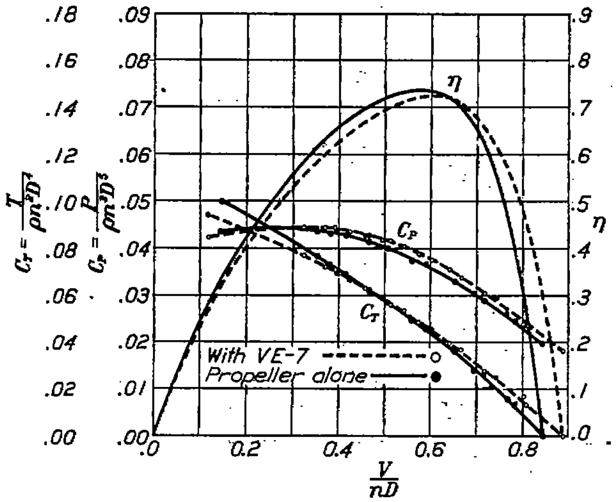

FIG. 25.—Model propeller B

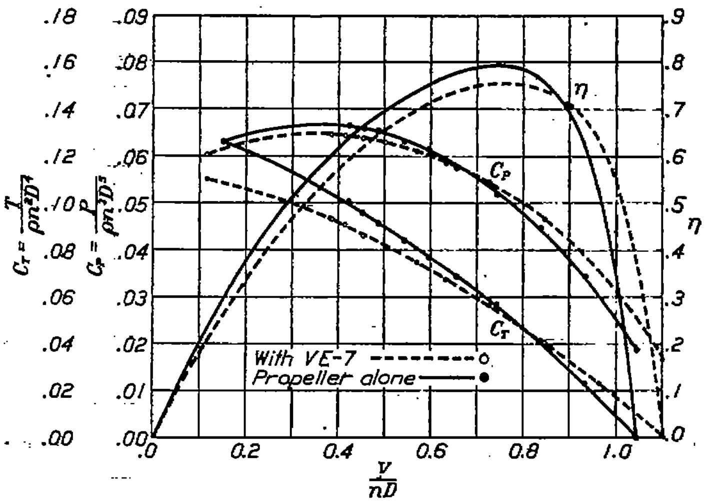

FIG. 26.—Model propeller D'

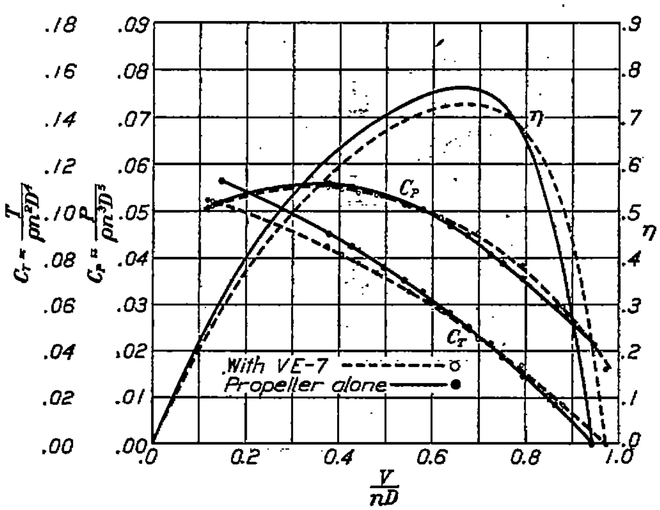

FIG. 27.—Model propeller I

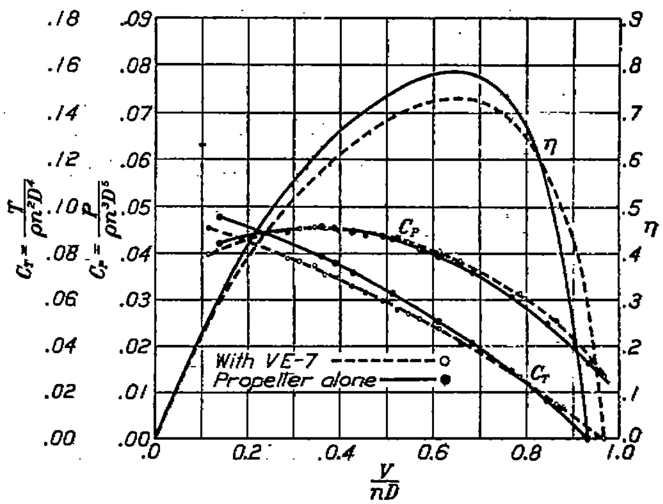

FIG. 28.—Model propeller K'

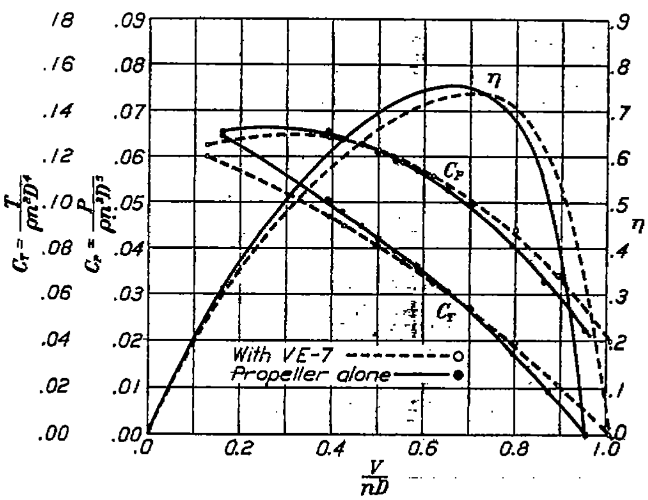

FIG. 29.—Model propeller L

(5) In consequence of these relative changes in the values of the thrust and power coefficients, it results that on the axis of V/nD the point of zero efficiency (for large values of V/nD) is carried to the right (larger values of V/nD) for operation with the model and that generally for large values of V/nD the propulsive efficiency is greater with the obstruction than with the propeller alone. On the other hand, for small or medium values of V/nD the propulsive efficiency for operation with the model is less than that for the propeller alone.

The two curves of efficiency thus cross and the point of equal values is seen to be, in general, at a value of V/nD somewhat larger than that for the maximum value on either curve.

Likewise it is seen that the maximum values of the propulsive efficiency for operation with the model are in all cases less than those for the propeller alone, and in particular that this loss in efficiency is carried over the range of values of V/nD from those for maximum value of efficiency along the direction of decreasing values (increasing slip). Due to limitations in diameter, it results in the normal case that propellers must be used over a range of values of V/nD, beginning with a large value somewhat less than that for maximum efficiency and extending over a small range in the direction of decreasing values. It thus follows that the air propeller in the normal practical case must be used over a segment of the efficiency curve beginning near but somewhat to the left (as here plotted) of the maximum value and extending to the left over a range of decreasing values of efficiency and hence over a range where the effect of an obstruction, as represented by the nose of the fuselage or other part of the airplane structure, will be to decrease the propulsive efficiency as compared with that for the propeller alone at the same value of V/nD.

(6) The amount of the loss in propulsive efficiency over the working range is seen to vary between some 3 and 5 per cent, and so far as these present observations indicate such loss is greater with high pitch ratio than with low and with narrow blades than with wide.

While these conclusions are in general agreement with those drawn from other similar investigations, the number of variant forms in the present research is too small to warrant the drawing of any final or definite general conclusions regarding the character of the relation between such loss in propulsive efficiency and the detailed characteristics of the propeller form.

TABLE I

GLIDE TESTS

Flight and run No.	Angle of glide path	Angle of wing	Angle of attack	Weight	Lift	Apparent drag	$1/2\rho V^2$	Specific weight of air	Velocity ft/sec.	R. P. M.	$\frac{V}{nD}$	Thrust	True drag	C_L	C_D
1-2	−6.2	3.9	10.1	2,070	2,058	223.6	9.60	0.0688	94.8	745	0.935	10.0	234	0.757	0.0861
1-3	−6.6	1.1	7.7	2,063	2,049	237.0	12.20	.0688	106.9	830	.946	9.1	246	.594	.0712
1-4	−6.6	−0.3	6.3	2,056	2,042	236.3	14.80	.0688	117.7	965	.896	34.7	271	.487	.0646
1-5	−7.6	−2.8	4.8	2,049	2,031	271.1	19.10	.0688	133.6	1,110	.892	48.9	320	.376	.0591
1-6	−9.2	−5.7	3.5	2,042	2,016	326.5	23.90	.0688	149.6	1,200	.916	39.6	366	.297	.0540
1-7	−10.0	−7.6	2.4	2,035	2,004	353.3	28.80	.0688	164.1	1,300	.928	35.7	389	.246	.0476
1-8	−11.2	−9.2	2.0	2,028	1,989	393.9	33.80	.0688	177.9	1,415	.924	47.7	442	.208	.0462
1-9	−13.2	−11.2	2.0	2,020	1,967	461.1	35.80	.0688	183.0	1,500	.897	83.3	544	.194	.0536
2-1	−6.0	−5.1	11.1	2,070	2,059	216.3	9.10	.0691	92.0	740	.914	15.8	232	.798	.0900
2-2	−6.8	1.7	8.5	2,063	2,049	244.3	12.10	.0702	105.8	820	.945	9.2	253	.598	.0739
2-3	−8.5	−4.1	4.4	2,056	2,033	303.9	22.80	.0702	142.9	1,180	.890	56.7	361	.322	.0671
2-4	−9.8	−6.2	3.6	2,049	2,019	348.7	27.50	.0714	157.5	1,300	.891	69.6	419	.259	.0538
2-5	−11.6	−8.7	2.9	2,042	2,000	410.7	34.30	.0714	175.9	1,420	.910	63.7	475	.206	.0489
2-6	−14.3	−12.0	2.3	2,035	1,972	502.6	43.20	.0725	195.7	1,580	.910	78.6	581	.161	.0475
22-2	−7.4	7.7	15.1	2,070	2,053	266.6	6.76	.0695	79.1	624	.932	7.5	274	1.070	.1430
22-3	−5.8	3.9	9.7	2,066	2,055	208.9	9.62	.0700	94.0	752	.919	15.1	224	.754	.0822
22-4	−6.7	−0.1	6.6	2,062	2,048	204.6	12.74	.0702	108.1	828	.959	4.4	209	.568	.0579
22-5	−6.9	−2.1	4.8	2,058	2,043	247.2	16.11	.0702	121.5	976	.915	27.0	274	.447	.0600
22-6	−7.1	----	----	2,054	2,038	253.9	19.91	.0705	134.8	1,100	.900	43.6	298	.361	.0528
23-2	−10.0	----	----	2,069	2,037	359.2	25.50	.0701	153.0	1,192	.943	21.0	380	.282	.0526
23-3	−11.3	----	----	2,064	2,024	404.3	30.20	.0700	166.6	1,336	.917	48.5	452	.236	.0528
23-4	−13.5	----	----	2,059	2,002	480.6	36.60	.0702	183.2	1,436	.938	35.6	516	.193	.0498
23-5	−15.4	----	----	2,054	1,981	545.8	43.40	.0717	197.4	1,532	.947	31.0	577	.161	.0469
24-2	−7.1	7.1	14.2	2,070	2,054	255.8	6.45	.0697	77.2	576	.985	−22.2	234	1.123	.1280
24-3	−6.1	5.6	11.7	2,066	2,054	219.6	7.28	.0695	82.1	656	.920	11.1	231	.996	.1120
24-4	−5.9	3.3	9.2	2,062	2,051	212.2	8.99	.0695	91.2	744	.901	19.2	231	.806	.0909
24-5	−6.0	1.6	7.6	2,058	2,047	215.1	10.39	.0698	97.9	792	.908	20.0	235	.696	.0799
24-6	−7.1	0.0	7.1	2,054	2,038	253.7	12.20	.0698	106.1	860	.907	23.6	278	.589	.0805
25-2	−6.9	−1.1	5.8	2,070	2,055	248.6	14.30	.0697	114.9	892	.946	10.6	259	.507	.0640
25-3	−7.4	−2.5	4.9	2,066	2,049	266.1	16.30	.0698	122.5	960	.938	15.8	282	.444	.0611
25-4	−7.6	−3.2	4.4	2,062	2,044	272.8	18.50	.0698	130.6	1,024	.937	18.6	291	.390	.0555
25-5	−8.0	−4.5	3.5	2,058	2,038	286.5	20.50	.0699	137.4	1,064	.949	13.1	300	.351	.0517
25-6	−8.8	−5.4	3.4	2,054	2,030	314.3	22.50	.0703	143.5	1,103	.952	12.6	327	.318	.0513
26-2	−8.1	−6.4	1.7	2,070	2,049	291.6	25.20	.0709	151.3	1,216	.914	41.5	333	.287	.0466
26-3	−11.2	−9.0	2.2	2,066	2,027	401.2	29.90	.0711	164.5	1,316	.918	46.9	448	.239	.0529
26-4	−13.1	−11.1	2.0	2,062	2,008	467.3	36.90	.0714	182.4	1,436	.934	39.6	507	.192	.0485
26-5	−15.0	−13.5	1.5	2,058	1,988	532.6	42.90	.0718	196.1	1,592	.906	86.1	619	.163	.0509
26-6	−15.4	−13.2	2.2	2,054	1,980	545.8	47.00	.0710	206.3	1,664	.911	90.6	637	.149	.0478

TABLE II

POWER FLIGHT DATA

PROPELLER B′

Flight and run No.	Specific weight, pounds per ft.³	V feet per second	R. P. M.	α Angle of flight path	Angle of attack	W	L	D	T	HP.	V/nD	C_T	C_P	η
6-2	0.0748	84.4	1,604	12.6	9.6	2,069	1,916	214	666	174	0.372	0.0771	0.0487	0.589
6-3	.0748	97.0	1,627	11.1	7.3	2,064	1,953	228	625	175	.421	.0702	.0468	.632
6-4	.0746	111.5	1,672	9.7	5.5	2,059	1,994	259	603	181	.471	.0641	.0447	.675
8-2	.0744	125.4	1,704	8.2	4.3	2,054	2,011	290	582	185	.521	.0600	.0435	.719
6-5	.0724	79.1	1,608	12.5	11.8	2,069	1,901	212	661	168	.348	.0785	.0434	.565
8-3	.0721	113.8	1,688	9.4	6.3	2,064	1,992	248	581	175	.476	.0628	.0433	.691
8-4	.0720	146.5	1,764	4.5	3.3	2,059	2,032	354	515	184	.587	.0505	.0401	.739
8-5	.0728	174.9	1,872	0	2.1	2,054	2,046	481	481	197	.658	.0395	.0350	.730
8-6	.0718	197.0	1,928	−5.1	1.5	2,049	2,044	589	400	198	.724	.0307	.0333	.667
8-7	.0765	0	1,620							180	0		.0477	.0

PROPELLER D′

Flight and run No.	Specific weight, pounds per ft.³	V feet per second	R. P. M.	α Angle of flight path	Angle of attack	W	L	D	T	HP.	V/nD	C_T	C_P	η
11-2	0.0733	874.1	1,648	12.6	12.9	2,070	1,860	218	670	174	0.345	0.1038	0.0687	0.521
11-3	.0737	7.7	1,684	11.2	9.1	2,066	1,945	218	618	178	.399	.0911	.0656	.554
11-4	.0739	102.4	1,664	9.6	5.8	2,062	1,983	238	582	177	.471	.0877	.0674	.613
11-5	.0737	121.4	1,670	7.2	4.7	2,058	2,015	280	538	178	.557	.0806	.0672	.668
11-6	.0742	134.4	1,704	5.6	3.7	2,054	2,027	320	520	182	.603	.0765	.0648	.718
31-2	.0741	72.4	1,608	14.9	13.8	2,070	1,817	229	761	168	.345	.1026	.0707	.501
31-3	.0747	86.2	1,612	13.3	12.3	2,065	1,862	214	690	169	.410	.1095	.0700	.641
31-4	.0745	103.7	1,640	11.5	6.4	2,060	1,970	240	651	171	.484	.1001	.0672	.720
31-5	.0747	116.9	1,660	9.7	4.9	2,055	1,992	269	615	173	.539	.0922	.0657	.756
31-6	.0747	131.1	1,688	7.5	3.9	2,050	2,012	310	578	177	.595	.0837	.0641	.777
31-8	.0765	0.0	1,650	0.0						178	0		.0675	.00
32-1	.0762	167.5	1,800	0.0	2.2	2,075	2,073	464	464	192	.713	.0579	.0559	.738
32-2	.0746	148.0	1,724	4.3	3.2	2,070	2,052	352	507	180	.657	.0704	.0611	.757
32-3	.0749	162.6	1,780	1.7	2.8	2,065	2,040	433	494	187	.700	.0642	.0571	.787
32-4	.0745	179.5	1,808	−2.0	1.9	2,060	2,049	513	441	188	.761	.0551	.0557	.761
32-5	.0792	199.5	1,888	−5.0	1.6	2,055	2,051	582	403	182	.804	.0504	.0505	.802
32-6	.0707	205.2	1,908	−6.5	1.4	2,050	2,041	626	394	187	.824	.0471	.0494	.786
32-7	.0698	206.4	1,896	−6.8	1.3	2,045	2,034	634	392	184	.835	.0481	.0501	.802
32-8	.0757	171.2	1,808	0.0	2.0	2,040	2,039	480	480	193	.726	.0598	.0560	.775
9-2	.0709	81.5	1,660	11.0	11.7	2,069	1,914	216	611	172	.375	.0964	.0684	.528
9-3	.0714	88.6	1,670	10.1	9.3	2,064	1,953	218	580	174	.407	.0898	.0674	.542
9-4	.0710	102.0	1,680	8.9	7.5	2,059	1,978	229	547	175	.466	.0841	.0677	.580
9-5	.0715	114.7	1,700	7.5	5.5	2,054	2,005	259	527	177	.517	.0786	.0653	.622
9-6	.0715	130.0	1,720	5.2	4.2	2,049	2,021	298	484	179	.579	.0705	.0640	.638
12-2	.0735	155.2	1,728	1.9	2.7	2,070	2,068	395	464	185	.689	.0655	.0632	.714
12-3	.0734	166.8	1,828	0.0	2.3	2,065	2,062	437	487	193	.699	.0549	.0560	.685
12-4	.0734	184.5	1,850	−2.4	1.8	2,062	2,044	532	446	194	.764	.0548	.0542	.772
12-5	.0731	197.0	1,892	−4.8	1.5	2,058	2,053	600	428	197	.798	.0504	.0516	.779
12-6	.0765	0.0	1,640							182	.0		.0699	0

PROPELLER I

Flight and run No.	Specific weight, pounds per ft.³	V feet per second	R. P. M.	α Angle of flight path	Angle of attack	W	L	D	T	HP.	V/nD	C_T	C_P	η
4-2	0.0734	95.7	1,590	12.1	7.7	2,063	1,951	228	660	171	0.442	0.0915	0.0611	0.662
4-3	.0738	108.3	1,622	10.8	5.9	2,056	1,973	247	632	175	.491	.0847	.0582	.714
4-4	.0742	123.9	1,680	8.5	4.4	2,049	2,000	286	589	183	.543	.0732	.0551	.722
4-5	.0749	137.9	1,682	6.8	3.4	2,042	2,015	332	575	186	.599	.0699	.0549	.762
4-6	.0748	156.0	1,747	4.0	2.6	2,035	2,024	403	545	192	.657	.0622	.0506	.808
4-7	.0752	169.0	1,825	1.8	2.1	2,028	2,025	469	531	200	.682	.0562	.0460	.832
4-8	.0765	0	1,580							177	.0		.0617	.0
5-2	.0744	79.4	1,615	12.7	12.5	2,074	1,872	217	663	174	.361	.0876	.0586	.540
5-3	.0750	108.7	1,660	10.6	5.8	2,068	1,987	251	631	181	.481	.0794	.0558	.684
5-4	.0739	183.7	1,852	−2.0	1.8	2,062	2,062	530	458	195	.729	.0470	.0438	.781
20-1	.0740	167.5	1,798	0	2.2	2,074	2,072	450	450	192	.686	.0492	.0475	.710
20-2	.0707	81.5	1,580	10.6	11.1	2,069	1,927	215	595	161	.381	.0881	.0607	.553
20-3	.0705	96.1	1,584	10.3	8.0	2,064	1,965	225	594	160	.445	.0876	.0598	.652
20-4	.0700	111.3	1,616	9.2	5.9	2,058	1,989	249	578	162	.505	.0823	.0577	.720
20-5	.0701	126.2	1,664	6.6	4.5	2,054	2,011	284	520	167	.557	.0698	.0542	.717
20-6	.0704	140.5	1,680	4.9	3.5	2,049	2,025	327	502	170	.614	.0658	.0531	.760
20-7	.0740	169.5	1,808	−0.3	2.1	2,044	2,043	461	450	193	.689	.0485	.0463	.722
20-8	.0765	0	1,600							178	.0		.0588	.0
21-1	.0725	171.0	1,764	−0.6	2.2	2,074	2,072	459	437	184	.712	.0504	.0486	.738
21-2	.0704	155.9	1,720	2.4	2.7	2,069	2,061	384	471	175	.665	.0589	.0513	.752
21-3	.0704	170.5	1,776	0	2.3	2,064	2,062	446	446	180	.706	.0522	.0483	.763
21-4	.0704	187.0	1,808	−3.3	1.7	2,059	2,055	523	405	183	.770	.0458	.0463	.752
21-7	.0720	178.0	1,804	−0.6	2.1	2,044	2,043	467	446	187	.704	.0496	.0467	.747

TABLE II—Continued

POWER FLIGHT DATA—Continued

PROPELLER K′

Flight and run No.	Specific weight, pounds per ft.³	V feet per second	R. P. M.	α Angle of flight path	Angle of attack	W	L	D	T	HP.	V/nD	C_T	C_P	η
14-2	0.0694	79.5	1,736	11.3	11.8	2,069	1,908	218	623	169	0.337	0.0775	0.0491	0.532
14-3	.0678	93.0	1,732	10.5	8.8	2,064	1,953	220	596	164	.394	.0763	.0488	.616
14-4	.0673	111.5	1,768	8.5	6.2	2,059	1,994	246	550	167	.464	.0681	.0474	.666
14-5	.0684	125.8	1,792	7.0	4.7	2,054	2,002	277	527	171	.514	.0625	.0459	.700
14-6	.0679	142.5	1,808	4.7	3.6	2,049	2,028	326	494	172	.580	.0580	.0452	.744
14-7	.0765	0	1,740							192	.0		.0501	.0
15-2	.0677	164.0	1,852	2.0	2.6	2,069	2,063	404	477	175	.650	.0535	.0427	.814
15-4	.0667	192.0	1,964	−3.4	1.8	2,069	2,066	525	402	182	.7175	.0407	.0379	.770
15-5	.0692	204.5	1,984	−6.8	1.4	2,064	2,054	610	367	192	.7575	.0351	.0374	.710
29-1	.0760	167.8	1,916	0	2.2	2,074	2,072	465	465	204	.643	.0434	.0402	.694
29-2	.0745	145.2	1,832	3.8	3.1	2,069	2,054	359	496	190	.582	.0517	.0435	.692
29-3	.0738	163.0	1,924	0.8	2.4	2,064	2,061	430	459	197	.623	.0439	.0396	.695
29-4	.0729	181.0	1,972	−2.9	1.9	2,059	2,043	511	407	198	.674	.0374	.0371	.680
29-5	.0732	195.0	1,960	−6.1	1.5	2,054	2,050	596	412	189	.731	.0378	.0361	.766
29-6	.0728	201.5	2,004	−7.0	1.4	2,049	2,038	622	372	199	.739	.0331	.0359	.681
29-7	.0760	170.0	1,916	0	2.1	2,044	2,043	476	476	204	.652	.0444	.0404	.716
30-1	.0764	168.0	1,916	0	2.2	2,075	2,073	468	468	205	.645	.0434	.0403	.694
30-2	.0748	76.7	1,768	14.2	11.5	2,070	1,871	210	718	186	.319	.0800	.0476	.536
30-3	.0746	90.6	1,744	13.1	8.3	2,065	1,928	219	687	182	.382	.0788	.0486	.620
30-4	.0751	104.9	1,772	11.4	6.2	2,060	1,970	243	650	187	.434	.0718	.0471	.662
30-5	.0756	120.0	1,788	9.4	4.6	2,055	1,998	279	615	189	.492	.0664	.0460	.710
30-6	.0756	134.0	1,848	7.2	3.6	2,050	2,017	322	579	195	.533	.0584	.0431	.722
30-7	.0763	169.5	1,940	0	2.1	2,045	2,044	474	474	206	.641	.0478	.0389	.788
13-1	.0765	0	1,720							191	.0		.0518	.0

PROPELLER L′

Flight and run No.	Specific weight, pounds per ft.³	V feet per second	R. P. M.	α Angle of flight path	Angle of attack	W	L	D	T	HP.	V/nD	C_T	C_P	η
18-1	0.0744	161.1	1,640	0.0	2.4	2,074	2,070	426	426	176	0.722	0.0554	0.0567	0.705
18-2	.0734	80.8	1,460	10.6	10.8	2,069	1,933	215	595	153	.406	.0990	.0706	.568
18-3	.0727	92.7	1,476	9.8	8.3	2,064	1,967	223	574	155	.462	.0944	.0697	.626
18-4	.0726	108.1	1,492	8.0	6.1	2,059	2,000	247	534	155	.532	.0844	.0675	.665
18-5	.0726	124.6	1,544	6.0	4.5	2,054	2,025	286	465	161	.593	.0699	.0632	.656
18-6	.0735	140.0	1,595	4.1	3.3	2,049	2,032	336	482	167	.645	.0671	.0588	.736
18-7	.0743	164.5	1,660	0	2.3	2,044	2,042	438	439	177	.728	.0559	.0549	.741
18-8	.0765	0	1,490							163	.0		.0680	.0
19-1	.0742	162.5	1,684	0.8	2.4	2,074	2,071	431	460	181	.710	.0570	.0537	.754
19-2	.0723	155.1	1,632	2.4	2.7	2,069	2,061	390	477	170	.699	.0648	.0589	.796
10-3	.0729	170.1	1,692	−0.3	2.2	2,064	2,062	458	447	179	.739	.0558	.0532	.775
10-4	.0742	179.5	1,746	−2.7	1.9	2,059	2,057	510	413	188	.756	.0475	.0500	.718
19-7	.0739	167.5	1,680	0	2.2	2.044	2.042	450	450	180	.732	.0562	.0541	.760

/

TABLE III

FINAL ADJUSTED COEFFICIENTS, FULL SCALE TESTS

PROPELLER B′

V/nD	C_T	C_P	η
0.30	0.0839	0.0493	0.510
.35	.0790	.0486	.568
.40	.0737	.0475	.620
.45	.0678	.0461	.662
.50	.0617	.0441	.700
.55	.0553	.0420	.723
.60	.0485	.0395	.737
.65	.0418	.0370	.735
.70	.0340	.0340	.700

PROPELLER D′

0.30	0.1070	0.0690	0.465
.35	.1013	.0687	.517
.40	.0960	.0680	.564
.45	.0906	.0673	.605
.50	.0850	.0662	.642
.55	.0798	.0648	.677
.60	.0740	.0630	.705
.65	.0679	.0605	.728
.70	.0615	.0576	.746
.75	.0550	.0545	.757
.80	.0485	.0510	.760
.85	.0416	.0471	.750

PROPELLER I

0.30	0.0999	0.0611	0.490
.35	.0948	.0608	.545
.40	.0900	.0600	.600
.45	.0842	.0588	.644
.50	.0786	.0573	.685
.55	.0728	.0555	.720
.60	.0663	.0532	.748
.65	.0595	.0507	.762
.70	.0520	.0475	.765
.75	.0447	.0443	.756
.80	.0372	.0404	.736

PROPELLER K′

0.30	0.0822	0.0495	0.498
.35	.0783	.0490	.560
.40	.0744	.0482	.618
.45	.0698	.0472	.665
.50	.0649	.0462	.703
.55	.0593	.0447	.730
.60	.0530	.0430	.740
.65	.0466	.0409	.739
.70	.0400	.0385	.727
.75	.0329	.0357	.690

PROPELLER L′

0.30	0.1060	0.0710	0.450
.35	.1030	.0710	.508
.40	.0995	.0705	.565
.45	.0950	.0698	.612
.50	.0896	.0685	.655
.55	.0829	.0662	.688
.60	.0755	.0634	.716
.65	.0678	.0600	.786
.70	.0596	.0560	.744
.75	.0504	.0512	.738

TABLE IV

TEST DATA—MODEL PROPELLERS ALONE

PROPELLER B′

No.	$\frac{1}{2}\rho V^2$	V	R. P. M.	T	Q	V/nD	C_T	C_{P_1}
1	2.642	47.71	1085	0.0	0.705	0.844	0.0	0.0196
2	3.106	51.90	1273	1.323	1.207	.782	.0134	.0245
3	2.610	47.42	1188	1.323	1.124	.766	.0153	.0260
4	3.114	52.02	1391	2.977	1.694	.718	.0260	.0289
5	2.638	47.73	1320	2.977	1.618	.694	.0279	.0304
6	3.200	52.59	1550	5.292	2.394	.651	.0362	.0329
7	3.218	52.88	1722	8.269	3.275	.590	.0458	.0365
8	2.714	48.45	1664	8.269	3.131	.559	.0488	.0371
9	2.764	48.95	1856	11.907	4.187	.506	.0565	.0399
10	2.894	50.10	2071	16.207	5.371	.464	.0619	.0412
11	3.578	55.79	2569	26.790	8.550	.417	.0686	.0428
12	3.074	51.63	2613	26.790	8.925	.380	.0728	.0430
13	3.164	52.39	2841	33.075	10.620	.354	.0762	.0434
14	.281	15.63	2101	26.790	5.807	.143	.0998	.0435

PROPELLER D′

1	3.096	51.90	1035	0.0	0.395	1.045	0.0	0.0184
2	3.083	51.78	1157	1.323	.922	.932	.0226	.0343
3	3.063	51.79	1285	2.977	1.452	.839	.0411	.0447
4	3.128	52.17	1463	5.292	2.229	.742	.0564	.0519
5	3.178	52.58	1665	8.269	3.182	.656	.0681	.0572
6	3.335	53.89	1885	11.907	4.357	.596	.0766	.0612
7	3.440	54.75	2106	16.207	5.605	.542	.0835	.0630
8	3.367	54.14	2319	21.474	7.054	.486	.0909	.0652
9	3.456	54.86	2532	26.790	8.445	.452	.0955	.0657
10	3.538	55.50	2745	33.075	10.037	.422	.1003	.0664
11	.360	17.70	2444	33.075	7.565	.161	.1260	.0629

PROPELLER I

1	2.435	45.28	959	0.0	0.504	0.945	0.0	0.0215
2	3.213	52.28	1210	1.323	1.094	.864	.0171	.0296
3	3.510	54.75	1377	2.977	1.651	.795	.0298	.0346
4	2.502	45.96	1225	2.977	1.479	.760	.0372	.0387
5	3.569	55.21	1524	5.292	2.373	.725	.0433	.0406
6	2.669	48.20	1423	5.292	2.243	.678	.0506	.0449
7	3.352	53.48	1674	8.268	3.290	.639	.0560	.0466
8	3.402	53.87	1864	11.910	4.397	.578	.0650	.0502
9	2.768	49.00	1813	11.910	4.173	.540	.0698	.0513
10	3.816	57.22	2317	21.170	7.137	.494	.0752	.0531
11	3.948	58.26	2729	33.070	10.203	.427	.0849	.0548
12	2.907	49.61	2630	33.070	9.704	.377	.0900	.0553
13	.353	17.42	2363	33.070	7.470	.147	.1132	.0635

PROPELLER K′

1	3.191	50.85	1090	0.0	0.515	0.933	0.0	0.0163
2	3.245	52.96	1252	1.323	.963	.846	.0162	.0247
3	3.366	53.94	1403	2.977	1,498	.768	.0290	.0306
4	3.348	53.90	1574	5.292	2.197	.684	.0410	.0357
5	3.411	54.30	1777	8.269	3.070	.611	.0503	.0390
6	3.479	55.10	2156	14.920	4.909	.511	.0622	.0429
7	3.042	51.28	2389	21.168	6.308	.429	.0712	.0445
8	2.992	50.86	2618	26.790	7.710	.389	.0751	.0452
9	3.051	51.29	2850	33.075	9.252	.360	.0781	.0455
10	.377	18.02	2577	33.075	6.965	.140	.0963	.0420

PROPELLER L′

1	3.042	50.31	1053	0.0	0.633	0.956	0.0	0.0221
2	2.992	49.94	1143	1.323	1.036	.874	.0188	.0326
3	3.065	50.53	1268	2.977	1.670	.796	.0343	.0403
4	3.141	51.22	1418	5.292	2.613	.722	.0458	.0505
5	3.092	51.55	1458	5.960	2.646	.704	.0531	.0493
6	3.227	51.91	1590	8.269	3.416	.653	.0607	.0525
7	3.227	51.92	1766	11.790	4.544	.588	.0717	.0567
8	3.339	52.87	1964	16.207	5.824	.538	.0782	.0588
9	3.533	54.38	2174	21.168	7.834	.500	.0833	.0605
10	3.582	54.83	2366	26.790	8.933	.464	.0893	.0624
11	3.645	55.31	2620	35.278	11.169	.422	.0959	.0636
12	3.686	55.81	2862	44.000	13.590	.390	.1009	.0653
13	.368	17.63	2188	33.075	7.955	.161	.1287	.0651

TABLE V

TEST DATA—MODEL PROPELLERS WITH MODEL VE-7

PROPELLER B′

No.	$\frac{1}{2}\rho V^2$	V	R.P.M.	T	Aug.	Q	V/nD	C_T	C_{P1}
1	2.535	46.24	998	0.0	0.0	0.562	0.889	0.0	0.0180
2	2.937	50.16	1192	1.323	.160	1.026	.808	.0132	.0235
3	2.526	46.20	1107	1.323	.214	.948	.801	.0144	.0248
4	3.020	50.87	1317	2.977	.320	1.564	.742	.0248	.0293
5	2.500	45.96	1227	2.977	.358	1.436	.719	.0278	.0304
6	3.002	50.72	1457	5.292	.530	2.200	.668	.0363	.0337
7	2.530	46.26	1387	5.292	.570	2.120	.641	.0393	.0354
8	3.024	50.91	1627	8.269	.850	3.046	.601	.0454	.0374
9	2.600	46.98	1571	8.269	.908	2.956	.574	.0482	.0386
10	3.041	51.05	1806	11.910	1.150	4.042	.542	.0533	.0403
11	2.591	46.89	1751	11.910	1.221	3.951	.514	.0559	.0415
12	3.116	51.72	1909	16.210	1.610	5.167	.494	.0585	.0416
13	2.639	47.40	1955	16.210	1.663	5.033	.466	.0612	.0426
14	3.273	52.97	2221	21.170	2.120	6.457	.458	.0626	.0426
15	2.655	47.56	2153	21.170	2.121	6.215	.424	.0662	.0434
16	2.779	48.74	2370	26.790	2.729	7.612	.395	.0691	.0440
17	3.339	53.50	2629	33.070	3.340	9.284	.391	.0704	.0444
18	2.910	49.88	2588	33.070	3.307	9.128	.370	.0717	.0442
19	2.364	45.08	2670	37.490	3.754	9.728	.324	.0765	.0444
20	.137	11.12	1844	22.050	2.240	4.412	.116	.0940	.0421

PROPELLER D′

No.	$\frac{1}{2}\rho V^2$	V	R.P.M.	T	Aug.	Q	V/nD	C_T	C_{P1}
1	2.640	47.89	905	0.0	0.0	0.274	1.105	0.0	0.0166
2	2.714	48.61	1050	1.322	.204	.701	.965	.0232	----------
3	2.709	48.68	1198	2.978	.409	1.335	.847	.0409	.0465
4	2.648	48.08	1378	5.293	.638	2.057	.728	.0563	.0548
5	2.613	47.75	1576	8.269	.985	2.898	.632	.0672	.0583
6	2.766	49.21	1798	11.910	1.418	3.929	.571	.0746	.0609
7	2.692	48.53	2015	16.210	1.873	5.074	.502	.0810	.0626
8	2.718	48.81	2243	21.170	2.420	6.375	.454	.0858	.0637
9	2.718	48.81	2453	26.800	3.040	7.688	.415	.0909	.0642
10	2.810	49.64	2686	33.080	3.859	9.284	.386	.0932	.0646
11	2.788	49.46	2688	33.080	3.808	9.273	.384	.0933	.0644
12	.181	12.54	2236	27.310	3.240	7.075	.117	.1100	.0602

PROPELLER I

No.	$\frac{1}{2}\rho V^2$	V	R.P.M.	T	Aug.	Q	V/nD	C_T	C_{P1}
1	2.455	45.80	942	0.0	0.0	0.360	0.972	0.0	0.0161
2	2.591	47.83	1087	1.323	.299	.851	.880	.0170	.0296
3	2.609	48.01	1213	2.977	.434	1.371	.792	.0340	.0383
4	2.639	48.34	1385	5.291	.698	2.100	.699	.0471	.0451
5	2.705	48.91	1582	8.270	1.012	2.956	.619	.0570	.0486
6	2.714	48.96	1783	11.910	1.365	3.944	.550	.0652	.0510
7	2.585	46.80	1949	16.210	1.735	5.037	.480	.0731	.0533
8	2.639	47.71	2170	21.170	2.231	6.301	.440	.0771	.0538
9	2.688	48.13	2379	26.790	2.763	7.708	.405	.0813	.0546
10	2.723	48.44	2591	33.070	3.441	9.236	.374	.0846	.0552
11	.086	8.55	1418	12.130	1.248	2.546	.127	.1040	.0510
12	.181	12.50	2094	26.680	2.775	5.545	.119	.1046	.0507

PROPELLER K′

No.	$\frac{1}{2}\rho V^2$	V	R.P.M.	T	Aug.	Q	V/nD	C_T	C_{P1}
1	3.037	51.61	1068	0.0	0.0	0.375	0.966	0.0	0.0134
2	2.644	47.34	1096	1.323	.402	.778	.864	.0145	.0256
3	3.098	52.16	1326	2.977	.613	1.343	.787	.0262	.0312
4	2.709	47.92	1455	5.513	.814	2.044	.659	.0418	.0381
5	3.138	52.53	1714	8.269	1.150	2.887	.613	.0474	.0402
6	2.548	47.08	1652	8.270	.982	2.752	.570	.0516	.0408
7	3.146	52.41	1917	11.690	1.483	3.812	.547	.0539	.0421
8	2.736	48.28	1855	11.910	1.478	3.745	.522	.0574	.0432
9	3.216	53.18	2165	16.210	2.045	4.971	.491	.0591	.0434
10	2.639	47.92	2105	16.260	1.813	4.793	.455	.0630	.0438
11	2.845	49.23	2317	21.170	2.569	5.987	.425	.0656	.0442
12	2.985	50.42	2545	26.900	3.093	7.340	.396	.0696	.0449
13	3.129	52.37	2848	33.070	3.843	8.969	.368	.0702	.0451
14	3.339	53.35	3094	41.900	4.268	11.003	.345	.0745	.0456
15	2.635	48.14	3091	41.900	4.624	10.530	.312	.0763	.0451
16	2.141	43.82	3062	41.900	4.579	10.181	.286	.0777	.0444
17	.217	12.83	2193	28.460	2.870	5.408	.117	.0903	.0397

PROPELLER L′

No.	$\frac{1}{2}\rho V^2$	V	R.P.M.	T	Aug.	Q	V/nD	C_T	C_{P1}
1	2.574	47.72	944	0.0	0.0	0.428	1.010	0.0	0.0198
2	2.399	45.16	1009	1.323	.191	.874	.895	.0210	.0340
3	2.447	45.67	1141	2.977	.314	1.437	.801	.0387	.0438
4	2.452	45.72	1304	5.292	.544	2.129	.701	.0529	.0497
5	2.447	45.78	1475	8.268	.889	3.033	.621	.0645	.0556
6	2.460	45.95	1660	11.910	1.272	4.037	.553	.0736	.0585
7	2.526	46.55	1857	16.210	1.713	5.274	.501	.0802	.0611
8	2.714	48.31	2270	26.790	2.784	8.180	.426	.0891	.0636
9	2.718	48.35	2466	33.070	3.395	9.722	.392	.0933	.0640
10	.177	12.37	1957	26.680	2.837	5.928	.127	.1199	.0623

TABLE VI

FINAL ADJUSTED COEFFICIENTS— MODEL PROPELLERS ALONE

PROPELLER B′

V/nD	C_T	C_P	η
0.30	0.0822	0.0441	0.559
.35	.0766	.0438	.612
.40	.0705	.0429	.658
.45	.0642	.0416	.697
.50	.0575	.0400	.718
.55	.0508	.0381	.733
.60	.0433	.0357	.735
.65	.0362	.0331	.711
.70	.0280	.0300	.653
.75	.0186	.0266	.525
.80	.0090	.0230	.313

PROPELLER D′

0.30	0.1128	0.0662	0.510
.35	.1073	.0665	.565
.40	.1020	.0665	.615
.45	.0960	.0658	.657
.50	.0896	.0646	.694
.55	.0832	.0630	.726
.60	.0761	.0607	.752
.65	.0696	.0584	.774
.70	.0623	.0553	.788
.75	.0547	.0518	.791
.80	.0468	.0478	.783
.85	.0382	.0430	.752
.90	.0291	.0380	.690

PROPELLER I

0.30	0.0958	0.0554	0.534
.35	.0934	.0557	.587
.40	.0875	.0554	.633
.45	.0814	.0545	.672
.50	.0749	.0532	.704
.55	.0683	.0518	.772
.60	.0616	.0492	.751
.65	.0540	.0462	.760
.70	.0460	.0426	.756
.75	.0377	.0388	.728
.80	.0288	.0349	.660
.85	.0192	.0304	.536
.90	.0093	.0261	.321

PROPELLER K′

0.30	0.0833	0.0451	0.554
.35	.0790	.0452	.611
.40	.0743	.0449	.659
.45	.0690	.0444	.700
.50	.0636	.0433	.734
.55	.0578	.0417	.762
.60	.0519	.0398	.780
.65	.0454	.0375	.786
.70	.0386	.0349	.774
.75	.0315	.0318	.742
.80	.0237	.0282	.672
.85	.0150	.0241	.528
.90	.0058	.0196	.266

PROPELLER L′

0.30	0.1110	0.0659	0.505
.35	.1045	.0654	.560
.40	.0979	.0642	.610
.45	.0912	.0628	.656
.50	.0848	.0608	.693
.55	.0770	.0586	.723
.60	.0692	.0558	.744
.65	.0612	.0527	.755
.70	.0523	.0490	.748
.75	.0434	.0448	.726
.80	.0339	.0400	.678
.85	.0237	.0347	.582
.90	.0127	.0294	.392

TABLE VII

FINAL ADJUSTED COEFFICIENTS— MODEL PROPELLERS WITH MODEL VE-7

PROPELLER B′

V/nD	C_T	C_P	η
0.30	0.0787	0.0444	0.531
.35	.0740	.0444	.583
.40	.0688	.0440	.627
.45	.0639	.0432	.666
.50	.0580	.0417	.695
.55	.0517	.0398	.714
.60	.0452	.0375	.724
.65	.0383	.0349	.714
.70	.0306	.0316	.678
.75	.0228	.0283	.606
.80	.0151	.0248	.487

PROPELLER D

0.30	0.1000	0.0644	0.466
.35	.0961	.0646	.521
.40	.0918	.0642	.572
.45	.0870	.0636	.616
.50	.0821	.0629	.653
.55	.0768	.0615	.687
.60	.0713	.0599	.714
.65	.0655	.0579	.735
.70	.0595	.0556	.749
.75	.0531	.0519	.763
.80	.0469	.0500	.750
.85	.0401	.0463	.736
.90	.0328	.0419	.708

PROPELLER I

0.30	0.0912	0.0550	0.498
.85	.0855	.0553	.548
.40	.0818	.0550	.595
.45	.0764	.0541	.636
.50	.0710	.0529	.671
.55	.0652	.0514	.698
.60	.0593	.0496	.717
.65	.0530	.0473	.728
.70	.0462	.0446	.725
.75	.0386	.0412	.709
.80	.0309	.0372	.666
.85	.0223	.0324	.586
.90	.0134	.0271	.445

PROPELLER K′

0.30	0.0774	0.0450	0.514
.35	.0730	.0451	.566
.40	.0687	.0450	.611
.45	.0640	.0443	.650
.50	.0590	.0432	.683
.55	.0541	.0420	.709
.60	.0489	.0406	.723
.65	.0430	.0383	.730
.70	.0373	.0361	.723
.75	.0310	.0333	.697
.80	.0241	.0301	.641
.85	.0172	.0263	.556
.90	.0102	.0217	.425

PROPELLER L′

0.30	0.1034	0.0648	0.478
.35	.0950	.0647	.530
.40	.0925	.0640	.578
.45	.0868	.0630	.620
.50	.0806	.0613	.658
.55	.0742	.0592	.689
.60	.0675	.0568	.713
.65	.0604	.0538	.729
.70	.0532	.0505	.737
.75	.0454	.0465	.732
.80	.0378	.0429	.705
.85	.0259	.0382	.643
.90	.0200	.0335	.587

TABLE VIII

ORDINATES FOR SECTIONS OF PROPELLER L'

Radius	10.89″		19.05″		27.22″	35.39″	43.55″	47.63″
Camber	Upper	Lower	Upper	Lower	Upper	Upper	Upper	Upper
Rad. L. E.	0.980″		0.32″		0.161″	0.104″	0.059″	0.038″
2.5	0.856	0.516	0.914	0.059	.660	.425	.245	.157
5	1.235	.738	1.316	.082	.947	.614	.350	.229
10	1.650	.986	1.761	.111	1.271	.820	.470	.304
20	1.990	1.192	2.117	.134	1.529	.986	.565	.366
30	2.088	1.251	2.228	.140	1.604	1.039	.594	.385
40	2.068	1.241	2.208	.140	1.594	1.029	.588	.382
50	1.990	1.192	2.117	.134	1.529	.986	.565	.366
60	1.816	1.091	1.940	.121	1.398	.905	.516	.336
70	1.548	.928	1.650	.104	1.189	.768	.441	.284
80	1.173	.702	1.248	.078	.901	.581	.333	.216
90	.732	.438	.781	.049	.562	.362	.209	.134
Rad T. E.	0.361″		0.16″		.123″	.080″	.045″	.029″

All ordinates in inches.
Stations in per cent of chord.

ORDINATES FOR SECTIONS OF PROPELLER K'

Radius	10.89″		19.05″		27.22″	35.39″	43.55″	47.63″
Camber	Upper	Lower	Upper	Lower	Upper	Upper	Upper	Upper
Rad. L. E.	0.784″		0.261″		0.108″	0.068″	0.039″	0.026″
2.5	0.571	0.343	0.611	0.036	.441	.248	.163	.106
5	.820	.493	.879	.055	.634	.408	.232	.153
10	1.101	.660	1.173	.072	.846	.549	.314	.205
20	1.323	.794	1.411	.088	1.019	.657	.376	.247
30	1.388	.836	1.483	.091	1.072	.692	.395	.259
40	1.379	.830	1.470	.091	1.062	.686	.392	.258
50	1.323	.794	1.411	.088	1.019	.657	.376	.247
60	1.209	.728	1.294	.078	.931	.604	.343	.226
70	1.029	.621	1.101	.068	.794	.513	.294	.192
80	.781	.467	.833	.052	.601	.389	.222	.145
90	.487	.294	.519	.033	.376	.242	.137	.091
Rad. T. E.	0.170″		0.120″		.082″	.052″	.029″	.020″

All ordinates in inches.
Stations in per cent of chord.

ORDINATES FOR SECTIONS OF PROPELLER I

Radius	10.89″		19.05″		27.22″	35.39″	43.55″	47.63″
Camber	Upper	Lower	Upper	Lower	Upper	Upper	Upper	Upper
Rad. L. E.	0.844″		0.272″		0.133″	0.087″	0.049″	0.033″
2.5	0.719	0.427	0.762	0.049	.550	.357	.204	.133
5	1.032	.615	1.097	.068	.789	.512	.291	.193
10	1.380	.822	1.470	.092	1.056	.686	.392	.259
20	1.661	.991	1.767	.112	1.271	.825	.471	.310
30	1.742	1.040	1.856	.117	1.337	.866	.495	.327
40	1.729	1.032	1.840	.117	1.326	.860	.490	.324
50	1.661	.991	1.767	.112	1.271	.825	.471	.310
60	1.522	.906	1.617	.109	1.165	.757	.430	.283
70	1.293	.770	1.377	.087	.991	.642	.367	.242
80	.930	.582	1.042	.065	.748	.487	.278	.182
90	.612	.365	.650	.041	.468	.305	.174	.114
Rad. T. E.	0.245″		0.120″		.108″	.068″	.038″	.024″

All ordinates in inches.
Stations in per cent of chord.

TABLE VIII—Continued

ORDINATES FOR SECTIONS OF PROPELLER D'

Radius	10.45″		18.28″		26.11″	33.94″	41.77″	45.69″
Camber	Upper	Lower	Upper	Lower	Upper	Upper	Upper	Upper
Rad. L. E.	0.877″		0.282″		0.128″	0.083″	0.047″	0.031″
2.5	0.686	0.410	0.730	0.047	.526	.338	.194	.128
5	.987	.589	1.053	.066	.758	.439	.279	.185
10	1.322	.790	1.410	.068	1.015	.655	.373	.247
20	1.583	.949	1.692	.106	1.222	.786	.448	.298
30	1.664	.996	1.777	.113	1.285	.830	.473	.313
40	1.654	.990	1.764	.113	1.275	.821	.470	.310
50	1.588	.949	1.692	.106	1.222	.786	.448	.298
60	1.454	.868	1.551	.097	1.118	.720	.410	.272
70	1.238	.739	1.319	.085	.952	.614	.351	.232
80	.937	.558	.936	.063	.720	.464	.266	.175
90	.586	.351	.623	.041	.451	.291	.166	.110
Rad. T. E.	0.26″		0.125″		.098″	.064″	.036″	.024″

All ordinates in inches.
Station in per cent of chord.

ORDINATES FOR SECTIONS OF PROPELLER B'

Radius	11.33″		19.83″		28.33″	36.83″	45.33″	49.57″
Camber	Upper	Lower	Upper	Lower	Upper	Upper	Upper	Upper
Rad. L. E.	0.952″		0.306″		0.139″	0.090″	0.051″	0.034″
2.5	0.745	0.445	0.792	0.051	.571	.367	.211	.139
5	1.071	.639	1.142	.071	.823	.530	.303	.201
10	1.435	.857	1.530	.095	1.102	.710	.405	.269
20	1.724	1.030	1.836	.115	1.323	.854	.486	.323
30	1.806	1.081	1.928	.122	1.394	.901	.513	.340
40	1.795	1.075	1.915	.122	1.384	.891	.510	.337
50	1.724	1.030	1.836	.115	1.326	.854	.486	.323
60	1.578	.942	1.683	.105	1.214	.782	.445	.296
70	1.343	.802	1.432	.092	1.034	.667	.381	.252
80	1.017	.605	1.081	.068	.782	.503	.289	.190
90	.636	.381	.676	.044	.490	.316	.180	.119
Rad. T. E.	0.250″		0.115″		.106″	.071″	.039″	.020″

All ordinates in inches.
Stations in per cent of chord

REFERENCE

1. W. S. Diehl: The Variation of Aerofoil Lift and Drag Coefficients with Changes in Size and Speed. N. A. C. A. Technical Report 111. 1921.